DIPARTIMENTO SCIENZE DELLA VITA

DOTTORATO DI RICERCA IN SCIENZE DELLA VITA

CICLO XXXV

COORDINATRICE Prof. ssa Simona Maccherini

Influenza and Respiratory Syncytial Virus: three approaches of methods Validation

SETTORE SCIENTIFICO-DISCIPLINARE: MED/42

TUTOR: Prof. Emanuele Montomoli

TUTOR aziendale: Dr. Alessandro Manenti

VisMederi srl

DOTTORANDO: Dr. Carolina Bonifazi

A.A. 2022-2023

INDEX

1. ABSTRACT

Influenza and Respiratory Syncytial viruses are the most common pathogens able to infect humans causing respiratory illness. They both have a high impact on the morbidity and mortality worldwide in particular for high-risk population. Influenza A and B viruses can have an impact in all the population, regardless the age of people, while respiratory syncytial virus is well known for its role in paediatric and geriatric respiratory infections. Given their high transmissibility, vaccination represents the most important tool to prevent repeated infections.

Candidate vaccines are administered during clinical trials phases in order to assess their immunogenicity and efficacy before to obtain the license. During this period, biological samples are collected from clinical trial participants and tested through different bioanalytical methods evaluating different, but required, parameters. Before to start clinical testing, the methods must be validated following ICH (International Conference on Harmonisation), FDA (Food and Drug Administration) or any other guideline required for regulatory submission. The validation process allows to define the method valid for its purpose and to guarantee the solidity of the analytical results. Parameters and acceptance criteria to be evaluated are different based on the applied technique and are defined by the different regulatory bodies.

The present work has been divided in three main tasks. The first one reports the validation process for flow cytometry for the evaluation of the immune response in human samples. The second one refers to the validation process of Real Time RT-PCR technique by using TaqMan technology for the detection and characterization of Influenza viruses by using viral RNA as starting template. The application of this technique allows to have a prediction of the efficacy of the candidate vaccine formulation. The third task includes the development and validation of the Microneutralization ELISA-based method for the detection and quantization of neutralizing antibodies against respiratory syncytial virus A and B subtype. The presence or absence of neutralizing antibodies allows to evaluate the immunogenicity of the new vaccines.

In general, acceptance criteria were fulfilled for each method analysed in the three tasks, demonstrating that the assays can be considered validated and subsequently applied for future clinical studies.

2. INFLUENZA VIRUS

2.1. Overview

Influenza viruses belong to the Orthomyxoviridae family, which includes negative-sense single-strand enveloped RNA viruses [1]. There are four types of influenza virus: A, B, C and D [2]. Influenza A virus is the most virulent pathogen in humans among all the four genera and it can cause the most severe disease. It can also infect birds and other mammals such as pigs, horses, canine animals and bats. Influenza B viruses can infect humans, pigs and seals, they evolve slower than A viruses and faster than C viruses [3]. However, it has been demonstrated that Influenza B viruses have a high impact on morbidity and mortality worldwide, especially in adolescents and children [4]. Influenza C viruses can infect humans and pigs, but they are associated with minor symptoms when compared to A and B viruses [5]. Influenza D viruses are known to infect cattle and pigs, but antibodies against the virus were found in human serum samples collected in Italy from 2005 to 2017, suggesting that it has the ability to infect and elicit an immune response in humans [6].

In humans the transmission is usually through respiratory droplets caused by cough and sneeze, but it can also occur through aerosol or surfaces contaminated by viruses. Generally, the symptoms affect the respiratory tract and coughing is the most common one [7]. Gastrointestinal symptoms may occur in children, accompanied by fever, chills, muscle pain, loss of appetite and confusion. In severe cases the infection may evolve into pneumonia, while in some cases it is asymptomatic [8].

The current nomenclature for Influenza A viruses involves natural host species, geographical origin, isolation year and strain number [9] as reported in Figure 1.

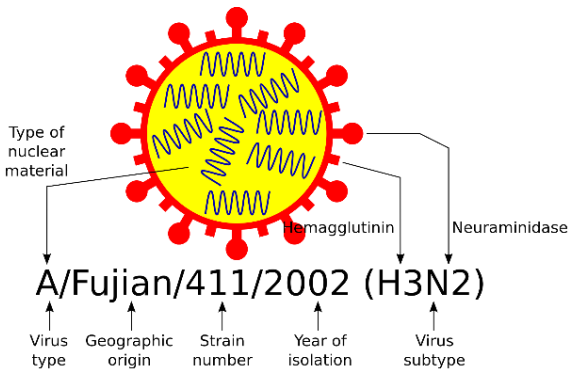

Figure 1: International nomenclature system for Influenza A viruses. The hemagglutinin and neuraminidase subtypes are reported in parentheses.

2.2. Structure

The Influenza viruses' genome consists of eight (Influenza A and B viruses) or seven (Influenza C and D viruses) segments of single-stranded negative-sense viral RNA encoding for 10 proteins [10].

Influenza A viruses are enclosed in a lipid membrane and divided into subtypes based on the two surface antigens, viral glycoproteins: hemagglutinin (HA) and neuraminidase (NA). HA is crucial for the recognizing and binding to sialic acids on carbohydrate side chains of cell-surface glycoproteins and glycolipids, while NA is important for the release of new virus particles. Two matrix proteins (M1 and M2) are included into the lipid membrane, playing a role in the stabilization and assembly of the virus (Figure 2) [11]. There are 18 different known HA antigens (H1 to H18) and 11 known NA antigens (N1 to N11), but only three types of HA (H1, H2 and H3) and two types of NA (N1 and N2) are commonly present in humans [12].

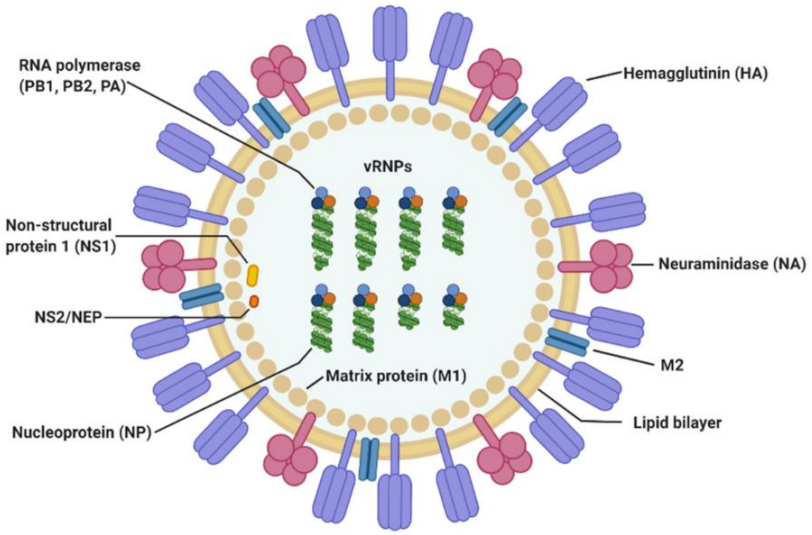

Figure 2: Influenza A virus structure reporting HA and NA antigens, M1 and M2 proteins, the lipid bilayer and the 8 RNA segments encoding for viral proteins.

Influenza B viruses were divided into two lineages, Victoria and Yamagata, based on the antigenic properties of hemagglutinin [13]. However, B/Yamagata-lineage circulation has not been confirmed since March 2020, therefore it is now considered extinct [14].

Influenza A viruses can undergo antigenic changes, which can occur in two different ways:

Antigenic drift: it consists of small point mutations in the genes of influenza viruses that can lead to changes in surface proteins HA and NA. These mutations can allow the new strain to partially avoid the immune response induced by previous strain, causing a new potential Influenza epidemic. Antigenic drift is also a primary reason why the composition of flu vaccines for use in the Northern and Southern Hemispheres is reviewed annually and updated as needed to keep up with evolving viruses [15].

Antigenic shift: the shift is an abrupt that can lead to a new HA and/or new HA and NA proteins in Influenza viruses that may infect humans for the first time. Basically, the shift can happen if a virus from animal population obtains the ability to infect humans. An example of the above-mentioned situation is what happened in 2009 when an H1N1 virus with genes from viruses originating from North American swine, Eurasian swine, humans and birds emerged to infect people and quickly spread, causing a pandemic [15].

2.2.1. Influenza virus antigens: HA and NA

Hemagglutinin (HA)

This glycoprotein is a trimer formed by three subunits consisting of two glycopeptides each, HA1 and HA2. Hemagglutinins recognize sialic acid present on cell-surface glycoconjugates but have limited affinity for them, and, as a consequence, virus attachment to cells requires their interaction with several virus HAs [16].

Initially, a single polypeptide chain (HA0) is synthetized in infected cells, which is then cleaved into two subunits, HA1 and HA2, linked by disulphide bonds. The cleavage of HA0 is fundamental for the glycoprotein to mediate the fusion between the viral envelope and host cell membrane. In details, HA1 domain binds sialic acid-containing cellular receptors at the top of the molecule while HA2 anchors the glycoprotein to the viral membrane (Figure 3) [17].

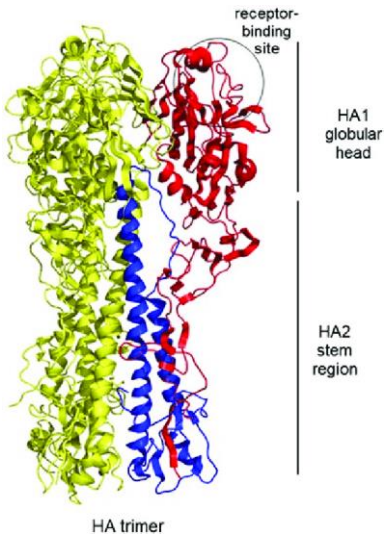

Figure 3: Structure of the influenza HA protein. The representative structure HA (H1 subtype) exists as a trimer on the virion surface and comprised the HA1 globular head (colored red on a single monomer) and the HA2 stem region (blue). The receptor-binding site is circled.

Neuraminidase (NA)

Viral neuraminidase removes sialic acids from both cellular receptors and newly synthetized HA and NA on nascent virions. NA cleavage of sialic acids prevents virion aggregation and stops virus binding back to the dying host cell via the HA, enabling the release of new virions and spread to new cell targets [18]. It exists as a tetramer of four identical monomers, consisting of four structural domains: the cytoplasmic tail, the transmembrane region, the stalk, and the catalytic head (Figure 4).

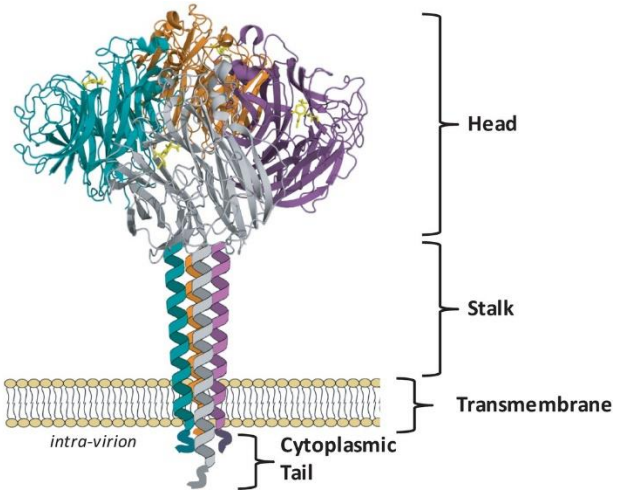

Figure 4: Structure of the influenza NA protein.

NA can have multiple roles in viral replication: it can enable movements of the virion through mucus [19], it can have a function in receptor binding especially for H3N2 strains and it facilitates the budding of new virions avoiding their aggregation [20].

2.3. Influenza virus replication cycle

Influenza viruses are able to replicate in live cells only. In humans, the primary targets are the epithelial cells located in the upper and lower respiratory tract. The Influenza virus life cycle can be divided into the following stages (Figure 5): entry into the host cell; entry of viral ribonucleoproteins (vRNPs) into the nucleus; transcription and replication of the viral genome; export of the vRNPs from the nucleus; and assembly and budding at the host cell plasma membrane [21].

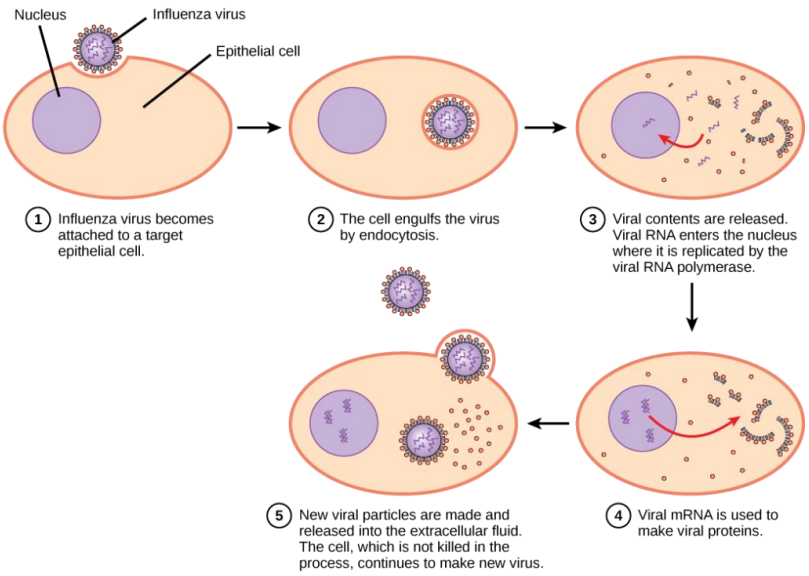

Figure 5: Infection, replication and release of new viral particles. 1) Viral attachment to the target cell mediated by HA. 2) The virus is brought into the target cell; this process is mediated by the low pH inside the endosome. 3) The virus loses its envelope and viral RNA is then released into cell nucleus, where replication process starts. 4) Assembly: M2 protein has a pivotal role in the formation of viral particles while the M1 protein is required during assembly and budding off of the viral particle. 5) New viral particles are released into the respiratory system from the infected cell.

<u>Entry into the host cell</u>

The HA binds the sialic acid residues on the surface of the host cell membrane. Two major linkages are found between sialic acids and the carbohydrates they are bound to in glycoproteins: α(2,3) and α(2,6). These are extremely important for the specificity of the HA molecules in binding to cell surface sialic acid receptors found in different species. Viruses from humans recognize the α(2,6) linkage, whereas those from avians and equines recognize

the α(2,3) linkages [21]. Upon the binding, receptor-mediated endocytosis occurs, and the virus enters the host cell in an endosome.

The fusion process is mediated by the low pH into the endosome, which is around 5-6 allowing the fusion of viral and endosome membranes. In particular, at low pH values a major conformational change in HA spike is induced and the subsequent exposure of HA2 peptide mediates the fusion. In addition, the acidic environment opens the M2 ion channel acidifying the viral core and permitting the release of vRNPs from M1 that can enter the host cell cytoplasm [22].

Entry of vRNPs into the nucleus

Viral transcription and replication occur in the nucleus, thus vRNP must enter the nucleus after being released into the cytoplasm [21].

Transcription and replication of the viral genome

Viral RNA segments are transcribed in mRNA by a transcriptase once entered into the nucleus. Once viral mRNA is transcribed, it is exported out of the nucleus and translated by host ribosomes in a cap-dependent manner to synthesize viral proteins [23]. New viral envelope proteins HA, NA and M2 synthesis starts in the cytosol, but the growing polypeptide chains are transported to the endoplasmic reticulum where proteins are glycosylated into trimmers and tetramers [7].

Assembly and budding at the host cell plasma membrane

After the vRNPs have left the nucleus, the virus has to form viral particles and leave the cell. Since influenza is an enveloped virus, it uses the host cell plasma membrane to form the viral particles that leave the cell and go on to infect neighboring cells. This last step generally occurs in the apical part of epithelial cells [22,23].

2.4. Influenza transmission

Influenza has a significative impact on public health, and it is responsible for high morbidity and mortality in humans, with annual attack rates up to 10% in adults and 30% in children [24]. In humans, the infection can be transmitted through breathing, talking, coughing, and sneezing mainly via aerosol and droplets [25]. Influenza is usually transmissible from one day

before the onset of symptoms to 5–7 days after. In healthy adults, the virus is shed for up to 3–5 days while in children and in immunocompromised patients, the virus may be transmissible for several weeks. Children aged 2–17 are considered to be the primary and most efficient spreaders of Influenza [26]. The World Health Organization (WHO) estimates that Influenza epidemics result in ~ 1 billion infections, 3-5 million cases of severe illness and 300 000-500 000 deaths every year [7].

2.5. Influenza epidemic

Influenza epidemic season occurs during the cold half of the year in each hemisphere. In tropical region it may occur throughout the year, causing outbreaks more irregularly. The magnitude of an epidemic depends on the preexisting population immunity, on the antigenic drift of the virus and on the virulence of the new virus variant [7].

2.6. Influenza pandemic

Influenza pandemics occur when a new strain of the Influenza virus is transmitted to humans from another animal species. These new strains are unaffected by any immunity people may have to the previous strains of human Influenza and can therefore spread extremely rapidly [27].

The first case of Influenza pandemic is dated on the year 1510 [28]. The major modern Influenza pandemics are listed in Table 1 [29].

Table 1: Influenza pandemics.

Name	Date	Subtype	Deaths worldwide
1889–1890 pandemic	1889-1890	H3N8/H2N2	1 million
Spanish Flu	1918-1920	H1N1	17-100 million
Asian Flu	1957-1958	H2N2	1-4 million
Hong Kong Flu	1968-1969	H3N2	1-4 million
1977 Russian Flu	1977-1979	H1N1	0.7 million
2009 swine Flu	2009-2010	H1N1/09	151 000-576 000

2.7. Influenza vaccine

Influenza vaccines are the most effective tools that protect against infection by Influenza viruses. New vaccine formulations are developed twice a year, as the Influenza viruses

rapidly change [30]. Vaccination is recommended yearly for high-risk groups of people as pregnant women, elderly, children between six months and five years of age, and those with health problems [31]. Seasonal Influenza vaccines for the 2022-2023 season are quadrivalent, they contain two strains from A viruses (H1N1 and H3N2) and two strains from B viruses (Victoria and Yamagata lineages) [32]. However, the WHO FluNet database showed Influenza B/Yamagata largely disappeared in 2021 and especially in 2022. Its detections resulted from the use of quadrivalent live-attenuated vaccines and it has been confirmed by the detection of B viruses post-March 2020, all ascribed to a lineage B/Victoria-lineage [14]. Different vaccines are licensed for use in different age groups and some of them are not recommended for some group of people [32].

Influenza vaccination can reduce the risk of hospitalization and death, vaccinated patients had a 26% lower risk of intensive care unit (ICU) admission and a 31% lower risk of death compared with those who were unvaccinated [33]. In addition, vaccination reduces children's risk of severe life-threatening Influenza by 75% [34].

Available Influenza vaccines are:

Standard-dose vaccine

It is manufactured using virus grown in eggs. These vaccines are approved for use in children as young as 6 months, most of them are given in the arm by a needle or jet injector [32].

Cell-based vaccine

It contains virus grown in cell culture, approved for people 6 months and older. This kind of vaccine is completely egg-free [32].

Recombinant vaccine

It is a completely egg-free vaccine made using recombinant technology and it is approved for use in people aged 18 years and older. It is made without Influenza viruses by including three times the antigen than other standard-dose inactivated vaccines. The advantage is the creation of a stronger immune response [32].

Egg-based high dose vaccine

It is approved for use in people aged 65 years and older. This vaccine contains four times the antigen than other standard-dose inactivated vaccines. The advantage is the creation of a stronger immune response [32].

Egg-based adjuvanted vaccine

It is approved for use in people aged 65 years and older. This vaccine contains an adjuvant that helps to create a stronger immune response [32].

Live attenuated nasal spray vaccine

It is made with attenuated (weakened) live Influenza viruses and approved for use in people aged 2 years through 49 years. It is not recommended for use in pregnant people, immunocompromised people, or people with certain medical conditions [32].

3. RESPIRATORY SYNCYTIAL VIRUS

3.1. Overview

Respiratory syncytial virus (RSV) is the most important respiratory tract pathogen of early childhood, its name is derived from the fusion between infected cells known as syncytia (Figure 6) [35, 36].

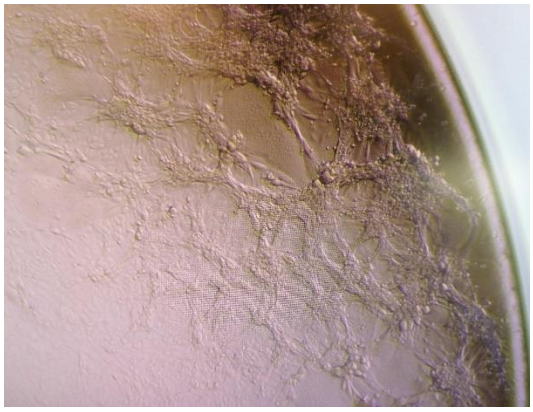

Figure 6: RSV-A syncytia observed in a well of a 96-wells plate in VERO cells.

It is the most common cause of respiratory hospitalization in infants, and reinfections are common in later life. Infections are typically prevalent during winter months and can cause bronchiolitis in infants, colds in adults and more serious respiratory symptoms in elderly and immunocompromised [37].

RSV is generally classified into two distinct subtypes, RSV-A and RSV-B, based on antigenic and sequence-based variations associated with attachment glycoprotein (G) [38]. Normally, both subtypes co-circulate during annual epidemics with a prevalence of RSV-A over RSV-B in most years [39].

Before the COVID-19 pandemic, RSV infections showed a seasonal trend in temperate regions, with peaks during winter months. Public health restrictions and social measures taken to mitigate the pandemic situation led to a significative reduction in RSV infections. However, on the other hand, restrictions contributed to increase the number of naïve subjects, especially naïve older children. After the relaxation of public health measures, an out-of-season outbreak of RSV infections occurred due to the accumulation of susceptible subjects. In opposition, a parallel increase in RSV infection in older adults was not observed,

suggesting that probably social measures have reduced infection rates in this age-group. [40].

3.2. Structure

RSV is a single-stranded, negative-sense RNA virus belonging to the *Paramyxoviridae* family, *Pneuomoviridae* subfamily and it is the only member of the genus *Pneumovirus* able to infect humans [35-38]. The genome contains 10 genes encoding for 11 proteins. The three surface viral proteins are the attachment glycoprotein (G), the fusion glycoprotein (F) and the small hydrophobic protein (SH) (Figure 7). The G and F proteins are crucial for the infectivity and pathogenesis of the virus; the first one enables the virus to attach to the respiratory epithelial host cells while the second one causes the fusion between the viral and host cell membrane and, in a later stage, the fusion of infected cells generating the syncytia.

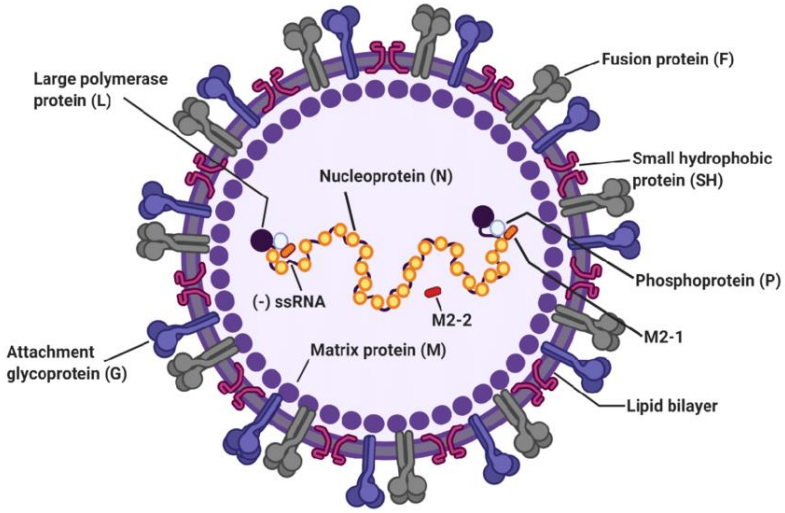

Figure 7: RSV structure.

M2-1 protein is the transcription processivity factor involved in genome transcription, RNA replication and particle budding. M2-2 protein is one of the responsible of the regulation of transcription and RNA replication [41].

3.2.1. RSV antigens: G, F and N proteins

<u>G glycoprotein</u>

The surface G glycoprotein is responsible for the viral attachment to host cells. The backbone contains 289-299 amino acids, depending on the strain, and is palmitolayed [42]. It has no sequence homology with other paramyxovirus attachment proteins, and no

hemagglutinating or neuraminidase functions. G glycoprotein is fundamental in host cell attachment and modulation of host immunity. It has been revealed that this protein has a CX3C chemokine motif that can bind CX3CR1 and regulate CXCL1-mediated responses. Furthermore, the central region of the G protein contains a highly conserved 13-amino acids domain followed by a highly basic heparin-binding domain (HBD). HBD is a possible attachment site to heparan sulfate (HS) found on the surface of most cells (Figure 8A). A peptide from the G protein HBD can bind to HEp-2 cells and inhibit RSV infection. G glycoprotein also has two mucin-like domains close to the central region (Figure 8B), which are highly variable in sequence, making that protein the most variable RSV protein [43].

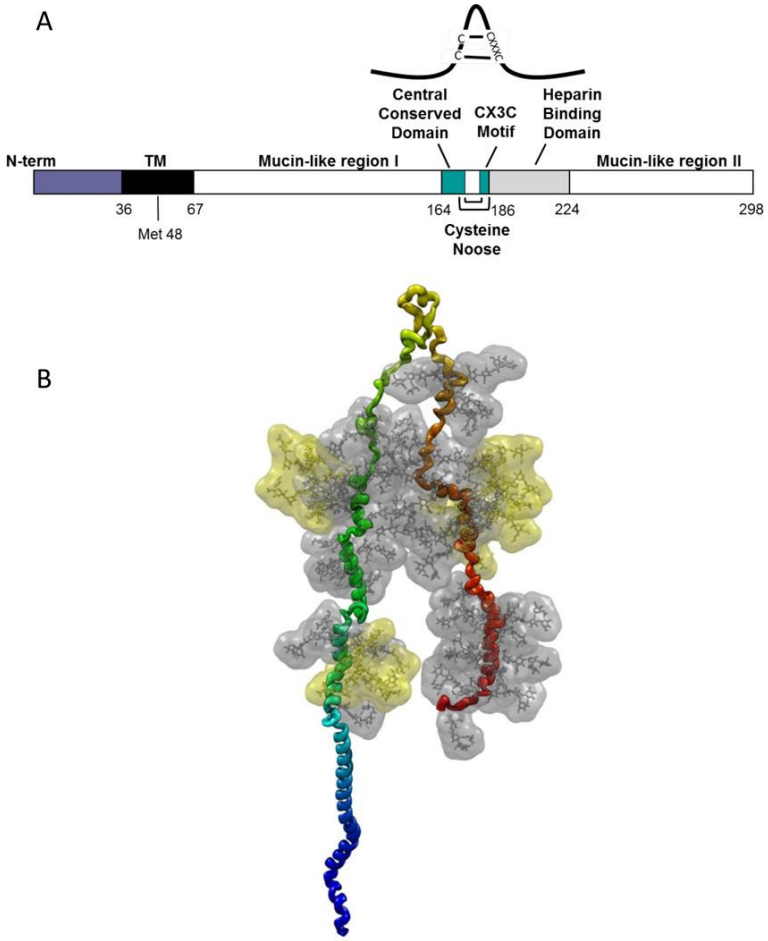

Figure 8: RSV G glycoprotein scheme. This is RSV A2 subtype G protein, consisting of two glycosylated mucin-like regions, separated by a central unglycosylated cysteine portion (yellow/green loop at the top of Figure B) stabilized by disulfide bonds.

F glycoprotein

The surface F glycoprotein is responsible for the fusion between the viral and host cell membranes, as well as syncytia formation between viral particles [41]. The F protein exists in two different conformations, a lollipop-shaped prefusion (preF) before virus-cell interaction and a crutch-shaped postfusion (postF) conformation (Figure 9). This last state exists due to the fusion between the viral and host cell membranes or due to unknown kinetic mechanisms that spontaneously switch the metastable preF conformation into the favorable postF one [44]. These two conformations are antigenically distinct and preF state has highly neutralization-sensitive antigenic sites that are not present on the postF conformation of the protein [45]. Therefore, it has been demonstrated that preF form can induce the majority of neutralizing antibodies following natural infection or immunization, making this antigen the first choice for vaccine development [46].

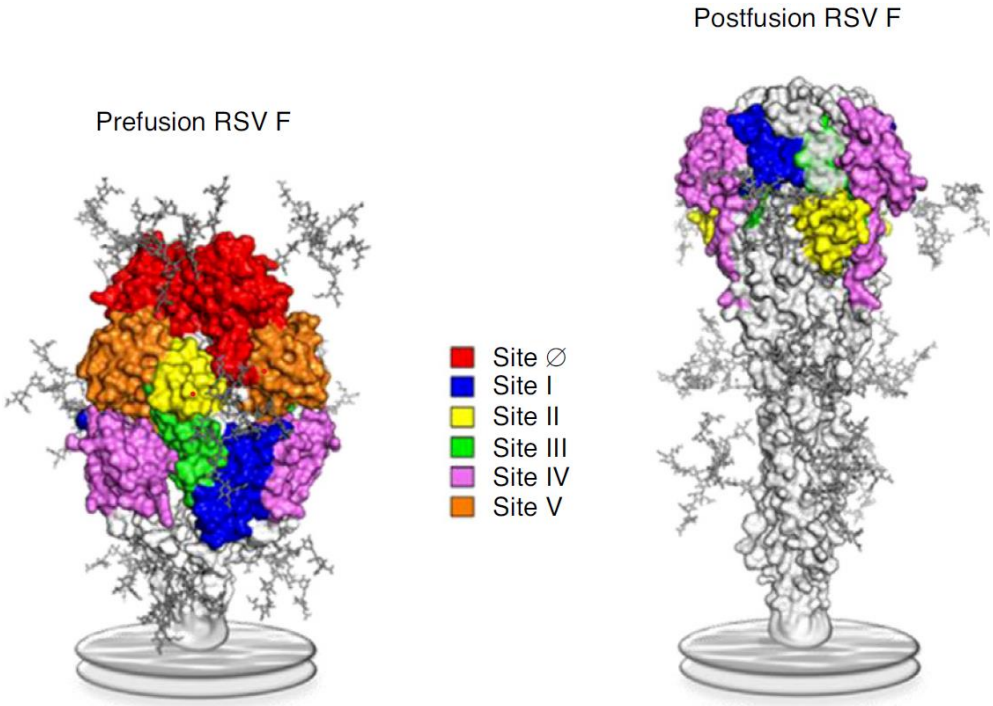

Figure 9: Different F glycoprotein conformations showing that the most neutralization sensitive epitopes only exist on the metastable preF conformation (Site 0, Site III, Site V). Once the F protein is trigged and undergoes the switch to the postF conformation, it is fixed and stable. However, the postF state induces a high amount of non-neutralizing antibodies that can interfere with antibody access on preF conformation [45].

N nucleoprotein

RSV RNA genome is coated by the viral nucleoprotein N to form the nucleocapsid (NC), which serves as the template for RNA synthesis by the viral RNA-dependent RNA

polymerase. The NC is a flexible helix, with variable pitches and numbers of N-proteins per turn of the helix, that is able to protect viral RNA from cellular nucleases and recognition by the innate immune system [47].

3.3. RSV replication cycle

The replication cycle (Figure 10) begins when the attachment glycoprotein G binds to the chemokine receptor (CX3CR1) on the apical surface of epithelial cells, and the F protein mediates the entry of the nucleocapsid into the cytoplasm [48]. The nucleocapsid served as template to synthetize mRNAs and progeny genomes. After the replication of the viral genome, structural proteins are synthetized in the Golgi apparatus and then deposited in the host cell membrane. In the cytoplasm there is the assembly of new virion particles, before budding through the host cell membrane [49].

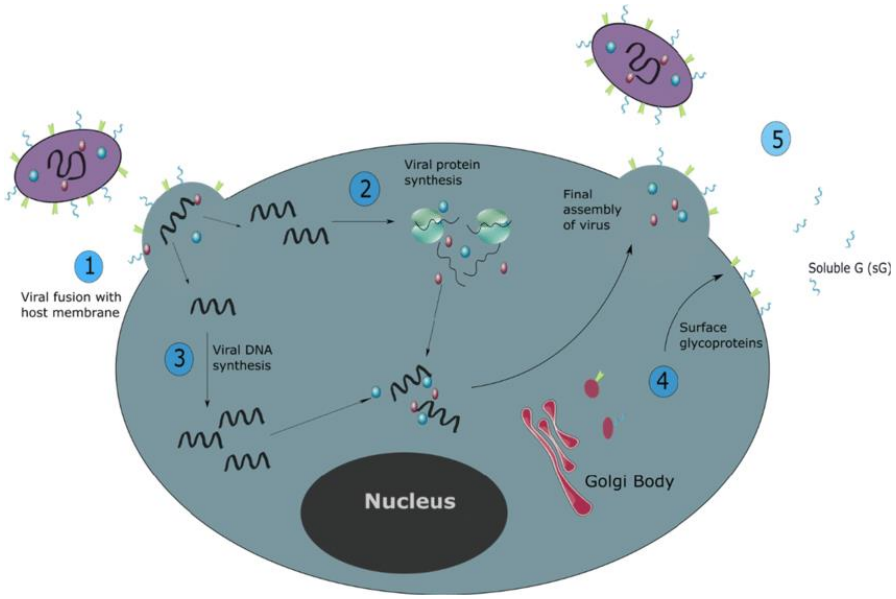

Figure 10: RSV replication cycle steps. 1) The virion binds to the host cell through G protein while F protein mediates membranes fusion. 2) Virus genome is used for proteins synthesis with a large amount of NS1/2 and sG proteins produced shortly after infection. These proteins can protect the replicating virus from the host immune defense. 3) The viral genome is replicated, and structural proteins are produced. 4) The surface glycoproteins are synthesized in the Golgi apparatus and transported in the host membrane. 5) Assembly of the new virion takes place in the cytoplasm, before budding through the host cell membrane.

3.4. RSV transmission

RSV is probably the most important respiratory tract pathogen of early childhood. It is estimated to cause around 33 million cases of disease and 66 000-199 000 deaths every year in children under 5 years of age worldwide. Most of children affected by the virus are aged 2 years or less and repeated infections can occur throughout life. In addition to children, the

virus can be also dangerous for older adults, patient with chronic disease and those with a compromised immune system [40]. The virus can spread through cough and sneeze, releasing droplets into the air, but also through contact with infected people. Once infected, people can be contagious for 3 to 8 days and in people having weakened immune system the virus can spread for up to 4 weeks [50].

The diagnosis can occur through different techniques, such as antigen testing, molecular testing and viral culture. The confirmation of RSV infection is not routinely recommended by the American Academy of Pediatrics (APP) because the bronchiolitis treatment is consolidated, but RSV diagnosis may be helpful in high-risk groups of people, for who the result can guide clinical decisions.

3.5. RSV epidemic

RSV infections are very common in children below the age of one year. For this age-group RSV infections represent the second cause of death globally after malaria, the first cause of death among respiratory infections and the first cause of hospitalization [51]. It is estimated that approximately the 90% of infants have experienced a RSV infection by the age of two years, and nearly all children have been infected by three years. However, the risk of death due to RSV infection occur in low-income countries having not access to basic supportive care [52].

For healthy young adults it is rare to develop severe illness from RSV, although the virus is a significative cause of morbidity and mortality in some groups of people, including elderly and those having lung and/or heart diseases. RSV can also be responsible for community-acquired pneumonias in a small percentage of adults [53]. Immunocompromised patients, both adults and children, are at particularly high risk to need hospitalization and to develop acquired pneumonias.

RSV seasonality can vary around the world. In most temperate regions, RSV infections typically start during the fall and peaks in the winter. Annual epidemics are generally caused by the presence of different subtypes; normally A and B subtypes co-circulate with a prevalence of RSV A subtype [53]. Public health restrictions taken in response to COVID-19 pandemic led to a significative decline in RSV infections, but there was also a rebound when lockdowns and restrictive measures were relaxed [54].

3.6. RSV vaccine

RSV vaccine development started in 1960s with the failure, in terms of protection and safety, of the first formalin-inactivated vaccine candidate that has overshadowed the research for almost 40 years [40]. Passive immunization was the main tool to prevent RSV infection and hospitalization in highest-risk infants. The most successful of human monoclonal antibodies (mAb) was Palivizumab [55]. This mAb is directed against the F glycoprotein of RSV, it was licensed in 1998 and it is effective in providing temporary prophylaxis against both RSV subtypes. Palivizumab can reduce hospitalization and death rates in infants having chronic lung disease, congenital heart disease and those born preterm. Anyway, its limitation is the cost which make it not usable in many parts of the world [56].

In May 2023 two different vaccines have been approved. The vaccine “Arexvy” made by the company GSK was approved by FDA for adults aged 60 and older, making it as the first RSV FDA-approved vaccine candidate [57]. The vaccine antigen is a stabilized form of RSV F protein. The vaccine “Abrysvo” made by the company Pfizer was approved by FDA in people 60 years of age and older. It is a bivalent recombinant protein subunit vaccine consisting of preF antigens belonging to both RSV subtypes [58].

Although the approval of these two new vaccines has been a significative step forward in the prevention of RSV, it is important to underline the role of neutralizing antibodies (nAb) in protecting against severe disease, as is supposed by evidence that high levels of nAb correlate with protection against RSV in adult volunteers [40].

4. VALIDATION OF A BIOANALYTICAL METHOD

Bioanalysis is an essential step in drug discovery and development starting from sample collection to sample analysis and data reporting. In order to obtain reliable results, an appropriate method should be applied demonstrating its fittingness by a series of parameters evaluation [59].

The main objective of the validation of a bioanalytical method is to demonstrate that it is suitable for its intended purpose. The most widely accepted guideline for method validation is the International Council of Harmonization (ICH) guideline Q2 (R2), applied for both pharmaceutical and medical sciences. This guideline provides an indication of the data that should be presented during a regulatory submission. All the obtained data collected during the validation of a method must be submitted to ensure the suitability of the procedure for the intended use and the reliability of the results. Different approaches from the ones included in the guideline may be applicable and acceptable with appropriate science-based clarifications, in addition, when an already established analytical method is used for a new purpose, validation testing can be reduced if scientifically acceptable [60].

A second guideline is represented by "M10 Bioanalytical Method Validation and Study Sample Analysis - Guidance for Industry" set by the Food and Drug Administration (FDA). Although the two guidelines are very similar, and FDA is a founding regulatory member of ICH, there could be some differences in the definition of limits for most parameters to be evaluated [61].

Validation parameters can differ based on the different bioanalytical methods; however, the most applied ones are specificity, linearity, accuracy, precision, range and robustness. For each parameter there are several criteria to be met in order to provide sufficient evidence that the bioanalytical method in exam fulfils its objectives.

Validation parameters are summarized in Figure 11.

Linearity

Dilution linearity is assessed to demonstrate that a high concentration of the sample of interest can be diluted to a concentration within the working range and still give a reliable result [62].

Relative accuracy

This parameter represents how close a measured value is to a standard value on relative terms. It can be evaluated by using either a conventional true value or an accepted reference value [60]. Relative accuracy is usually calculated by applying the formula: *100 x (observed value / expected value)*.

Precision

The Precision of an analytical procedure expresses the closeness of agreement between a series of measurements obtained from multiple sampling of the homogeneous sample under the prescribed conditions. Three aspects of precision parameter can be considered: repeatability, intermediate precision and format variability.

The intra-run variability or repeatability is the variation expected across replicates under the same operating conditions over a short period of time [60].

The intermediate precision is determined from the total variance component. It indicates the variations and random events that can occur within laboratories, such as days of experiments, environmental conditions, operators and equipment.

The format variability represents the variation expected across results yielded by multiple replicates in routine testing.

Specificity

The specificity is the ability of the assay to detect and distinguish the analyte of interest [61].

Robustness

The robustness of an analytical procedure is its capacity to remain unaffected by small but deliberate variations during measurements and gives an indication of its reliability.

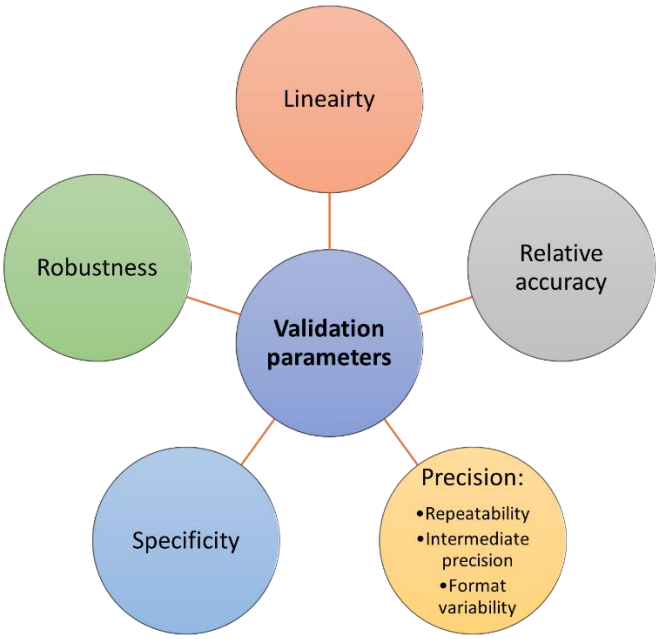

Figure 11: Validation parameters scheme.

5. CORRELATES OF PROTECTION

Although the definition of correlates of protection is still not defined, they can be classified as measurements of immune parameters that allow the estimation of the degree of protection against infection or disease induced by a pathogen. Considering this aspect, correlates of protection are essential in the development and licensure of vaccines [63].

Influenza virus

The correlate of protection which is normally accepted for Influenza is 1:40 hemagglutination inhibition (HI) titer, generally associated with a 50% protective ability [64]. HI assay is considered as the gold standard for evaluating Influenza vaccines as set by the FDA and European Medicines Agency (EMA) Committee for Medicinal Products for Human Use (CHMP). Anyway, there are several additional aspects that contribute to the efficacy of influenza vaccines, such as age of people and the type of immunogen. In this regard, it has been noted that there is a difference between young and elderly people because of IgG serum antibodies that correlate well only in people aged under 50 years [63, 65, 66].

A second serological assay recommended by CHMP is the single radial haemolysis assay (SRH), based on a passive haemolysis of erythrocytes mediated by complement and induced by the antibody-antigen complex. The haemolysis area is directly proportional to the concentration of anti-influenza antibodies in the serum [67]. A SRH area ≥ 25 mm^2 corresponds to the 70% and more of vaccine efficacy in adults aged 18-60 years and less than 60% in people over 60 years old [63, 67].

Virus neutralization assay is a sensitive and specific assay able to detect functional neutralizing antibodies able to block the viral attachment and entry in target cells [68]. Although the neutralization is an important function of antibodies, also antibody-dependent cellular cytotoxicity (ADCC) and antibody-dependent phagocytosis (ADP) play a key role in protection [63].

Influenza vaccines may also contain neuraminidase as antigen because it has an important role in reducing the morbidity and mortality limiting the spread to other target individuals [69]. Serological assays that can be applied to detect the presence of anti-neuraminidase antibodies are the Enzyme-Linked Lectin Assay (ELLA) and the ThioBarbithuric Assay (TBA).

All these serum assays are classically used to evaluate Influenza vaccine responses. Anyway, these methods are not able to provide precise correlates of protection, especially for non-traditional vaccine approaches that may rely to a greater extent on mucosal antibodies or cellular immunity for protection. Cell-mediated immunity (CMI) plays an important role in host immune response against Influenza illness and in the development of long-term immunological memory [70, 71].

Influenza vaccine efficacy can be supported the molecular biology, Real Time RT-PCR, showing the presence or absence of the target in a sample matrix [70].

Respiratory Syncytial Virus

The protection against RSV is more complex to be measured than the Influenza one since placentally transferred antibodies can prevent RSV infection and maternal immunization may reduce illness in young infants. Infant antibody titer against RSV-A is demonstrated to be three times higher than those against RSV-B and infants who remained healthy show higher RSV-A and B titers compared with infected infants. A study demonstrated that an RSV-A inhibitory concentration $(IC)_{80}$ titer > 239 or RSV-B titer > 60 at birth is associated with protection and decrease of pneumonia risk. Antibodies against the preF conformation of F glycoprotein are those that correlate best with protection [72].

The main correlate of protection are neutralizing antibodies with an increase in efficacy as the titer increase and, therefore, serological assays that can detect those antibodies are the gold standard [63, 73].

Anyway, although the major focus is on antibody-mediated protection, $CD4^+$ and $CD8^+$ T cells and innate cell responses can also act as correlates of protection [74].

6. AIM OF THE STUDY

The present work is divided in three main tasks:

1. The first task is based on the set-up and validation of flow cytometry to be applied for the evaluation of immune responses from samples collected during clinical trials. The aim of this part is to document the results obtained from the validation of the flow cytometry assay using fluorescent antibodies to characterize cell populations and their production of inflammatory markers (interleukins and cytokines) in human samples. The scope is to validate the method for the detection and quantization of IL-2, IL-13, CD40L, IFN-γ and TNF-α cell markers in specific live positive human cell populations, so that it could be applied for clinical trials performed for the evaluation of vaccines efficacy and immunogenicity.

2. The second task is focused on a proposal of validation approach for Real Time RT-PCR for the detection and characterization of Influenza virus strains. The scope is to demonstrate that this method is suitable for its intended use using extracted viral RNA as starting template and a TaqMan-based Real Time PCR assay. Evaluated parameters meet the acceptance criteria, therefore the method can be applied in clinical trials.

3. The third task represents the set-up and validation of high-throughput micro-neutralization assay for Respiratory Syncytial Virus A and B. The aim of this part is to provide a detailed validation process for the method in exam and to demonstrate that it can effectively support the immunogenicity and efficacy assessment of candidate vaccines and the definition of correlates of protection.

The three tasks composing this work have been completely carried out in VisMederi srl Laboratories in collaboration with the Department of Molecular and Developmental Medicine at the University of Siena.

7. TASK 1

7.1. Introduction

Cell-mediated and humoral immune responses evaluated in samples collected during clinical trials are crucial information supporting the efficacy of a candidate vaccine, medical drug substance or product. Therefore, a full characterization and validation process must be applied in order to provide consistent and reproducible data. Although several recommendations for the standardization of flow cytometry assay validation for its clinical application have been published by several organizations, such as the Flow Cytometry Action Committee of the American Association of Pharmaceutical Scientists (AAPS), so far harmonized guidelines are not available yet. This aspect is partly due to the lack of qualified reference materials, intrinsic cells variability, cells stability, bioanalytical category of the data, complexity of the method and of the data analysis [75, 76].

7.1.1. Cell-Mediated Immunity

The immune response can be divided into innate and adaptative responses. The innate immunity is the first line of defence to an intruding pathogen, it is non-specific, and it has no immunological memory [79]. The adaptative immunity is classified in cell-mediated immunity and antibodies -mediated immunity.

Cell-mediated immunity is a type of immune response that does not involve antibodies, while lead to activation of phagocytes, antigen-specific cytotoxic T-lymphocytes, and other cytokines in response to an antigen [80]. T-cells ($CD3^+$) are classified as $CD3^+/CD4^+$ (commonly abbreviated as $CD4^+$) and $CD3^+/CD8^+$ (commonly abbreviated as $CD4^+$) according to the expressed surface molecules. $CD4^+$ cells are also known as T helper cells (T_h cells) and their main role is the activation of B and T cells. In particular, Type 1 T_h cells (T_h1 cells) are able to produce interferon-gamma (IFN-γ), interleukin (IL)-2 and tumour necrosis factor-beta (TNF-β), which activate macrophages and are responsible for cell-mediated immunity and phagocyte-dependent protective responses towards pathogens. On the other hand, $CD8^+$ cells are known as cytotoxic T lymphocyte (T_c cells) due to their function of killing cancer cells, pathogen-infected cells, and damaged cells [81, 82]. T cells can recognize epitopes associated with the major histocompatibility complex (MHC) proteins. MHC gene complex codifies for the MHC I and MHC II proteins, responsible for presenting pathogen peptides to

the immune system. Generally, MHC I proteins present epitopes to T_c cells while MHC II proteins occur on antigen-presenting cells (APCs) (macrophages, B cells, dendritic cells).

7.1.2. Flow cytometry

Flow cytometry is a technology used to detect and measure single cells or particles, suspended in a buffered salt-based solution, as they flow past single or multiple lasers [77, 78]. The sample suspension is first pressurized and then injected into a tube, its speed is dependent on the fluid pressure in the tube (Figure 12-1). At the level of flow cell, laser beam and cells interact, and fluorescence signal emissions are detected with an optical collection system (Figure 12-2). When cell pass through the excitation source, the laser beam is refracted in all directions. A detector in front of the laser beam measures forward scatter (FS) light and several detectors to the side measure side scatters (SS) light (Figure 12-3). FS correlates with cells size, while SS is proportional to the granularity of the cells. Therefore, cell populations can be distinguished based on differences in their size and granularity. The detector converts analog measurements of FS and SS light as well as dye-specific fluorescence signals into digital signals that can be analysed by a computer software (Figure 12-4 and 12-5). The cell suspension is directed into a stream that allows to generate individual droplets (Figure 12-6). A droplet containing the cell or particle of interest is positively or negatively charged and pass through an electric field between two deflection plates, then is collected into an appropriate tube (Figure 12-7) [78].

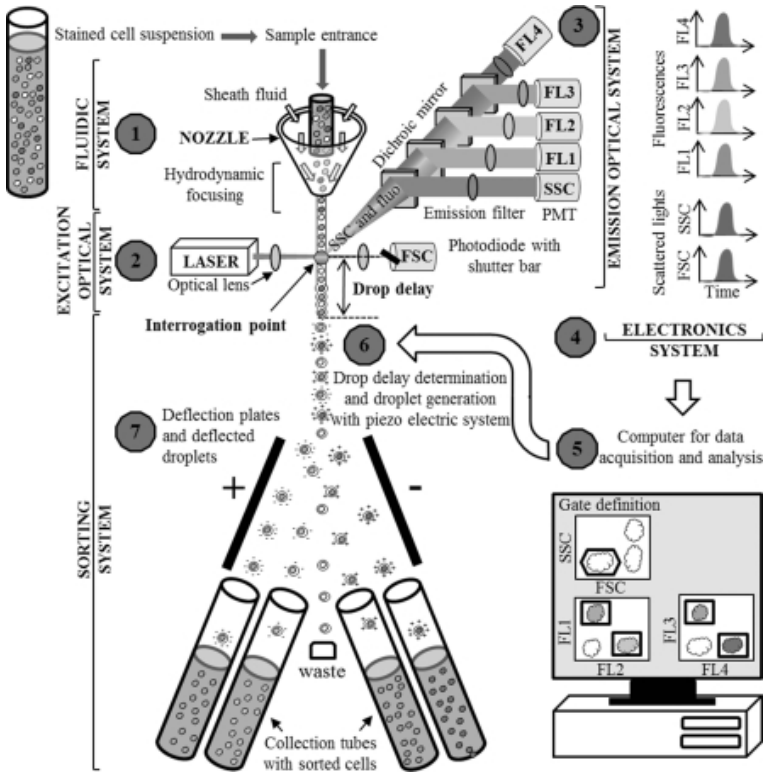

Figure 12: Schematic diagram of flow cytometry, from starting sample matrix to sorted cells.

Clinical trials aimed at evaluating vaccine immunogenicity are investing more and more on techniques involving the simultaneous and accurate measurements of subpopulation of stimulated peripheral blood mononuclear cells (PBMCs) and several extracellular and intracellular cytokines, chemokines, and cytotoxic activity by means of flow cytometry [71, 78, 79].

7.2. Materials and method

7.2.1. PBMCs thawing and stimulation

Commercially available PBMCs were purchased from CTL Europe GmbH. These cells were rapidly thawed (2 min) at 37°C and transferred in a 15 mL sterile tube containing pre-warmed thawing solution composed by PBS w/o Ca^{2+} Mg^{2+} (Gibco Life Sciences) with addition of 2.5 mM Ethylene Diamine Tetraacetic Acid (EDTA) (PanReacAppliChem) and 20 µg/mL Deoxyribonuclease I (DNAse I) (Sigma). The samples were washed twice by centrifugation at 311 g (rotor 75006441 K, 1203 RPM, radius 19.2 cm; *RCF = 11.2 x Radius x (RPM/1000)*^{2}) for 10 min at room temperature (RT) and then counted. PBMCs were resuspended in medium prepared as follow: RPMI-1640 medium with L-Glutamine (Gibco) with the addiction of 1% Foetal Bovine Serum (FBS) (Euroclone), 1% Penicillin/Streptomycin

100X (Euroclone), 1% Na pyruvate 100X (Gibco), 1% Non-essential amino acids 100X (Gibco), 1 µg/mL anti-CD28 (Purified NA/LE Mouse Anti-Human CD28, BD Biosciences) and 1 µg/mL anti-CD49d (BD Pharmingen™ Purified NA/LE Mouse Anti-Human CD49d, BD Biosciences). The latter two are co-stimulatory antibodies.

Positive control was prepared by incubating cells with complete medium supplemented with a stimulus, Staphylococcal enterotoxin B from *Staphylococcus aureus* (SEB) (Sigma-Aldrich) at the final concentration of 1 µg/mL. Negative control is prepared by incubating cells with complete medium only.

One million cells were cultured in a 96-well round bottom plate in complete medium and then overnight incubated for 16 hs at 37°C in humified atmosphere containing 5% CO_2. After 2 hs of incubation, Brefeldin A (BFA) (Sigma-Aldrich) was added in each well at the final concentration of 5 µg/mL. The addition of BFA results in enhanced detection of intracellular cytokines.

7.2.2. Flow cytometric analysis (FACS)

After overnight incubation, the plates containing PBMCs were centrifugated at RT at 699 g for 4 min. The supernatant was discarded and PBMCs were washed with 200 µl/well of PBS-2.5 mM EDTA and centrifuged at 699 g for 4 min. Cells were then stained with Live/Dead staining (ThermoFischer) 1:1000 diluted in PBS solution and incubated for 20 min at RT in the dark. Cells were then washed twice in PBS-2.5 mM EDTA and centrifuged at RT at 699 g for 4 min. After this process, the cells were permeabilized incubating them with 1X BD cytofix/cytoperm in the dark for 20 min at 4 °C, then washed twice with 1x perm/wash buffer in PBS-2.5 mM EDTA + 1% BSA and centrifuged at 699 g for 4 min at 4 °C (+2/+8 °C). To identify T cell subsets, the supernatant was removed and single-cell suspension was stained with the appropriate combination of the following directly conjugated monoclonal antibodies (MoAb) whose have been previously titrated to select their correct dilution: CD3 BV786 Clone SK7, CD4 BB700 Clone SK3, CD8 BV510 Clone RPA-T8, CD40L APC Clone TRAP1, IFN-γ A-700 Clone B27, TNF-α PE CY7 Clone MAb11, IL-13 BV421 Clone JES10-5A2 and IL-2 PE Clone MQ1-17H12 (BD Biosciences) diluted in perm/wash buffer. Perm/wash buffer was previously prepared diluting it in PBS-2.5 mM EDTA + 1% BSA + 2% normal rabbit serum. The cells were incubated with the mixture containing fluorescent antibodies for 20 min at RT in

the dark. Cells were then washed twice with perm/wash buffer 1x, centrifuged at 699 g for 4 min at RT, resuspended in PBS-2.5 mM EDTA and samples were acquired at the FACS machine (BD LSR II 4 LASER, interfaced to PC FACS Diva software 8.0.1 (BD Biosciences). A total of 500K events per sample were analysed and dead cells were excluded. Initial gating selected only live cells using an amine reactive dye (Live/Dead staining). The lymphocytes were gated using a drawn gate using SSC-A (granularity) and FSC-A (size). The single cells were selected using SSC-A and SSC-W gate. Subsequent gating allowed to select $CD3^+$ cells and within this $CD3^+$ lymphocyte gate, $CD4^+$ and $CD8^+$ T cells were identified (Figure 13). The number of $CD4^+$ and $CD8^+$ cells expressing each marker (IL-2, IL-13, CD40L, IFN-γ and TNF-α) was evaluated.

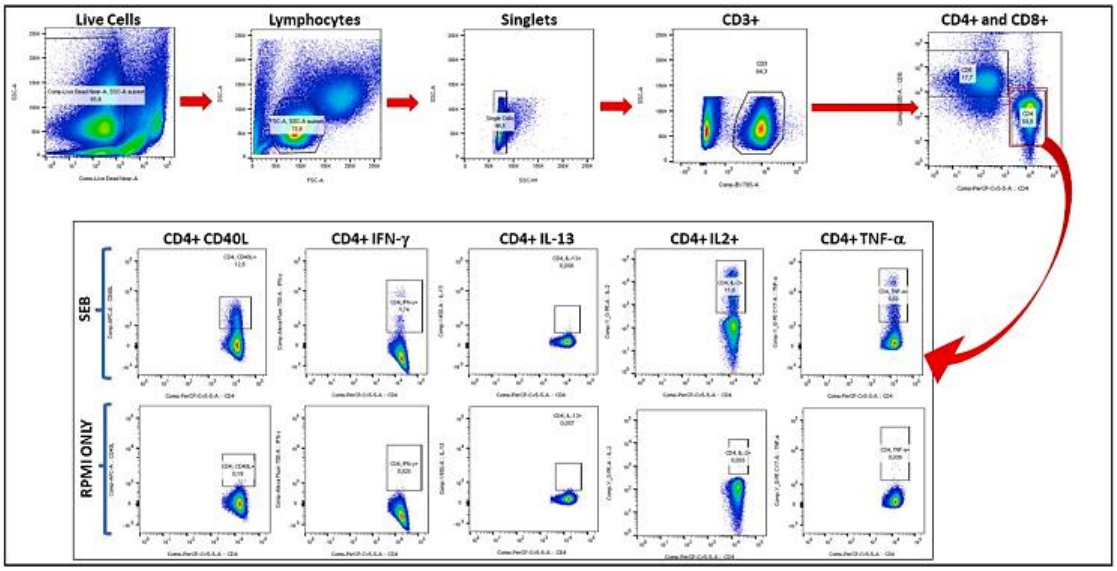

Figure 13: Gating strategy for flow cytometry-based evaluation of cytokine production in SEB-stimulated $CD4^+$ cells *vs* medium.

7.3. Validation parameters

The validation parameters evaluated included: range and detection limits, repeatability/intra-assay precision, intermediate precision, specificity, linearity and relative accuracy. The robustness was not evaluated due to the lack of fluorescent antibodies and commercial PBMCs.

The percentage of CD4 and CD8 positive cells for each marker was calculated *vs* the live cells population.

Range and detection limits

The detection and quantitation limits were defined by the technical characteristics of the assay. The Flow cytometer instrument can detect a single cell, set as Lower Limit of Quantitation (LLOQ); the layout of the experiment was supposed to include 1×10^6 cells for each well, and this value could be assumed as Upper Limit of Quantitation (ULOQ).
These assumptions lead to a range of detection and quantitation from 1 to 1×10^6 cells. A derived percentage values in terms of cells expressing marker *vs* the number of live cells could be calculated having a theorical range of 0.001%–100.000%.

Precision – Repeatability/Intra-assay

The intra-assay precision or repeatability was determined by one operator within one run. In detail, 6 repetitions (6 wells containing 1×10^6 cells from one characterized subject) were seeded, stimulated with SEB and stained with the full fluorescent antibody panel.
The percentage of coefficient of variation (CV%) calculated between positive cells for each marker among SEB-stimulated samples had to be ≤ 20%.

Precision – Intermediate precision

Intermediate Precision was determined as the variability across two operators across different runs (Day 1 and Day 2). In detail, 6 repetitions (6 wells containing 1-1x10^6 cells from one characterized subject) were seeded, stimulated with SEB. In addition, 6 repetitions of the same cells, without stimulants (negative), were included in each run. All the samples received a full antibody panel staining.
The CV% calculated between positive cells for each marker among SEB-stimulated samples and unstimulated ones, among the two operators had to be ≤ 20%.

Specificity

The specificity was evaluated on single cytokine-stained cells: once defined the correct dilution for each antibody, the specificity was assessed on the results of that specific dilution. In detail, one series of single-color staining (for each marker) was performed on SEB stimulated PBMCs, and the percentage of cells positive for each marker was calculated *vs* the live cell population. To evaluate the specificity, the same calculation was performed on markers not represented by the antibody used for the staining, this approach evidenced

non-specific fluorescence signals (e.g., Cells stained for CD40L were evaluated for IL-2, IL-13, IFN-ɣ and TNF-α).

The ratio between the percentage of specific marker cells and the percentage of non-specific marker cells had to be ≥ 10.

Linearity

Linearity was evaluated by spiking SEB-stimulated stained cells into unstimulated stained cells. In particular, SEB-stimulated stained cells were evaluated neat and mixed in a 50% (1:2), 25% (1:4), 12.5% (1:8), 6.25% (1:16), 3.13% (1:32), 1.56% (1:64) and 0.78% (1:128) ratio in unstimulated stained cells in order to obtain 2 replicates from one operator. Dilutional linearity samples were tested by two operators in two different days. The number of cells expressing each marker (IL-2, IL-13, CD40L, IFN-ɣ and TNF-α) was evaluated. The coefficient of determination (R^2) of the regression between the Log of Geometric Mean (GM) of the percentages of the 4 values obtained from the positive cells for each marker evaluated respect to the Log of sample dilution was calculated.

R^2 of the regression line had to be ≥ 0.95.

Relative Accuracy

For the evaluation of Relative Accuracy, the data of Dilutional Linearity were used and GM between replicates was calculated.

The GM of the obtained percentages for each marker had to be within 80–120% respect to the calculated value from the neat sample results. The applied formula was: *100*(GM Observed/GM Calculated)*.

7.4. Results

The chosen approach for validation experiments allowed different components contributing to the overall variability of the assay to be distinguished guaranteeing the flow cytometry assay for its dilutional linearity, relative accuracy, repeatability, specificity, intermediate precision, range, and detection limits.

7.4.1. Range and detection limits

The evaluation of the range and detection limits showed that all the acceptance criteria were met for all the cytokines.

However, a further clarification has been made for $CD4^+$ $IL\text{-}13^+$ and $CD8^+$ $IL\text{-}13^+$, since even for SEB-stimulated cells the number of positive cells for this marker was too low to be detected and therefore it was not comparable with the unstimulated condition.

The measurements on the unstimulated cells (blank) returned a mean of 0.009 and a standard deviation (SD) of 0.003. A bootstrap method with 100K resamples from normal distribution was used for estimating the threshold in the blank distribution which identifies the limit of detection (LOD). Assuming the following formula: *LOD = mean(blank) + 3.3xSD(blank)*, the threshold was calculated as the quantile of the normal distribution with probability (p) equal to 0.9995 (Figure 14 A).

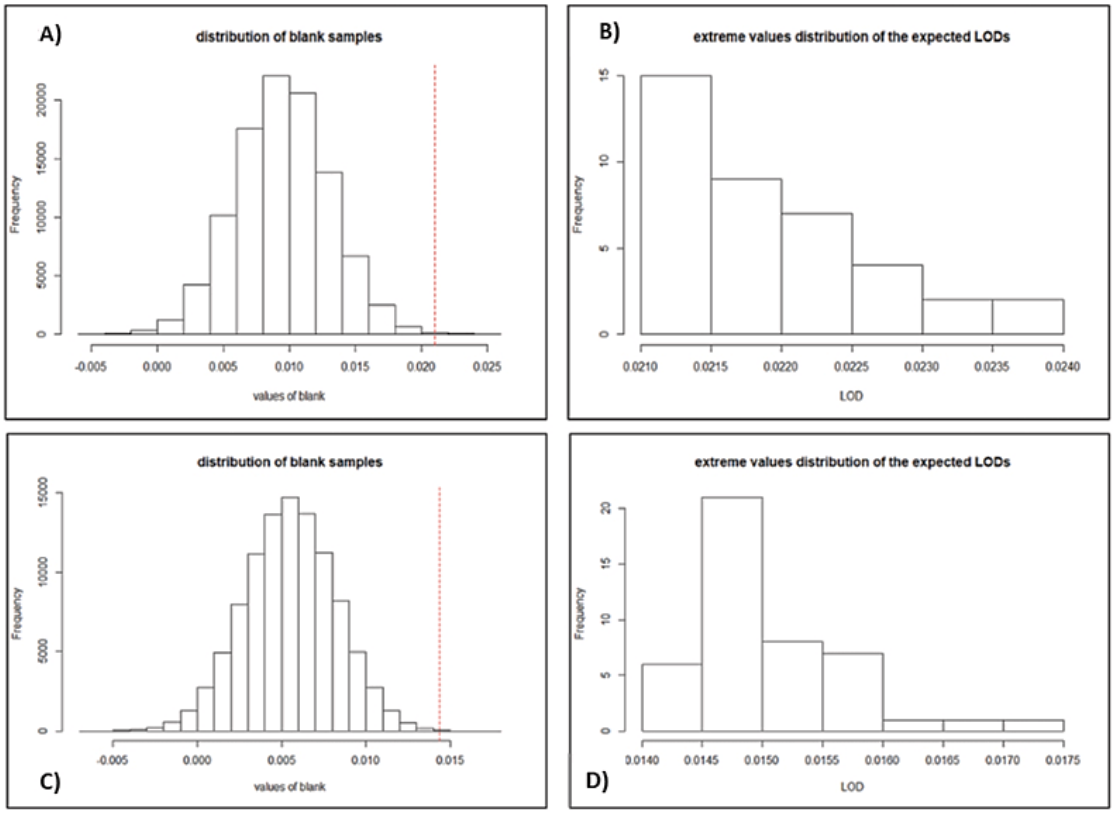

Figure 14: $CD4^+$ and $CD8^+$ $IL\text{-}13^+$ subpopulations: distribution of measurements over the blank for $CD4^+$ $IL\text{-}13^+$ (A); distribution of the extreme values of the LOD assuming normal distribution of blank samples for $CD4^+$ $IL\text{-}13^+$ (B); distribution of measurements over the blank for $CD8^+$ $IL\text{-}13^+$ (C); distribution of the extreme values of the LOD assuming normal distribution of blank samples for $CD8^+$ $IL\text{-}13^+$ (D).

The extreme values observed in the right tail of the distribution of the blank samples starting at the threshold value (red dotted line) equal to 0.021 constituted the distribution of the expected LOD values (Figure 14 B). The 99% confidence interval of the LOD distribution was in the range [0.021: 0.024]. From the measurements obtained on SEB-stimulated cells a

mean of 0.023 and a SD of 0.003 were calculated (Figure 14 B). When analyzing the IL-13 sample for the $CD8^+$ cells population a mean and a SD for the unstimulated cells equal to 0.005 and 0.003 were calculated, respectively. The bootstrap distribution of blank samples is reported in Fig. Figure 14 C. The lower limit of LOD (i.e., the threshold) was 0.014 and the 99% confidence interval of the LOD distribution was in the range [0.014: 0.017] (Figure 14 D). The returned a mean equal to 0.005 and a SD equal to 0.004 with an expected value below the threshold of the LOD distribution (Figure 14 C and D).

As for all fluorescent antibodies used in these validation experiments, also for IL-13 the choice of the optimal concentration to be used in the staining mix was previously chosen in a set-up experiment by calculating the Mean of Fluorescence Intensity (MFI) at different dilutions (from 1:20 to 1:320) (Table 2). The calculation of MFI allowed to choose 1:40 as the best concentration for IL-13 to be used in validation experiments.

Table 2: Calculation of MFI for $CD4^+$ IL-13^+ and $CD8^+$ IL-13^+.

		$CD4^+$			**$CD8^+$**		
Cytokine	**Dilution**	**Mean+**	**Mean-**	**Ratio**	**Mean+**	**Mean-**	**Ratio**
IL-13	1:20	757	770	0.983	794	737	1.077
IL-13	1:40	644	611	1.054	710	611	1.162
IL-13	1:80	577	600	0.962	669	597	1.121
IL-13	1:160	540	543	0.994	537	565	0.950
IL-13	1:320	487	510	0.955	509	502	1.014

7.4.2. Precision: intra-assay or repeatability

For the SEB-stimulated $CD4^+$ subpopulation, the assay met the acceptance criteria for repeatability for all the cytokines evaluated.

For the SEB-stimulated $CD8^+$ subpopulation, the assay was repeatable for all the cytokines evaluated except for IL-13. (Table 3).

Table 3: Repeatability results for $CD4^+$ and $CD8^+$ stimulated population.

$CD4^+$		**$CD8^+$**	
Samples	**CV%**	**Samples**	**CV%**
CD40L SEB	7.88%	CD40L SEB	2.36%
IFN-γ SEB	5.33%	IFN-γ SEB	7.39%
IL-13 SEB	16.83%	IL-13 SEB	33.25%

IL-2 SEB	5.72%	IL-2 SEB	12.65%
TNF-α SEB	2.09%	TNF-α SEB	4.66%

7.4.3. Precision: inter-assay or intermediate precision

For the SEB-stimulated $CD4^+$ population, the assay met the acceptance criteria for intermediate precision for all the cytokines evaluated.

Concerning the SEB-stimulated $CD8^+$ population, the assay met the acceptance criteria for intermediate precision for all the cytokines evaluated with the exception of IL-13. Results are reported in Table 4.

Table 4: Intermediate precision results for $CD4^+$ and $CD8^+$ stimulated population.

$CD4^+$		**$CD8^+$**	
Samples	**CV%**	**Samples**	**CV%**
CD40L SEB	9.03%	CD40L SEB	0.91%
IFN-γ SEB	1.80%	IFN-γ SEB	0.92%
IL-13 SEB	10.27%	IL-13 SEB	89.66%
IL-2 SEB	8.59%	IL-2 SEB	0.84%
TNF-α SEB	0.93%	TNF-α SEB	0.52%

7.4.4. Specificity

Concerning the specificity, when the denominator in the signal to noise (*s/n*) ratio obtained was equal to 0, the ratio could not be calculated, and the *s/n* was reported as "n/a".
For the $CD4^+$ population, the assay resulted to be specific for all the cytokines evaluated apart from cells stained for IL-13 and cross-evaluated for CD40L and IFN-γ. The IL-13 *s/n* ratio for CD40L and the IL-13 *s/n* ratio for IFN-γ were 1.389 and 0.568, respectively.

Concerning the $CD8^+$ population the assay was demonstrated to be specific for all the cytokines evaluated. Results are reported in Table 5.

Table 5: Intermediate precision results for $CD4^+$ and $CD8^+$ stimulated population.

$CD4^+$		**$CD8^+$**	
SEB-Stimulated $CD4^+$ stained for $CD40L^+$	***s/n* ratio**	**SEB-Stimulated $CD8^+$ stained for $CD40L^+$**	***s/n* ratio**
s/n ratio for IFN-γ	n/a	*s/n* ratio for IFN-γ	n/a

s/n ratio for IL-13	n/a	*s/n* ratio for IL-13	40.46
s/n ratio for IL-2	n/a	*s/n* ratio for IL-2	n/a
s/n ratio for TNF-α	9840.18	*s/n* ratio for TNF-α	n/a
SEB-Stimulated CD4⁺ stained for IFN-γ	***s/n* ratio**	**SEB-Stimulated CD8⁺ stained for IFN-γ**	***s/n* ratio**
s/n ratio for CD40L	1663.46	*s/n* ratio for CD40L	61.54
s/n ratio for IL-13	n/a	*s/n* ratio for IL-13	123.08
s/n ratio for IL-2	n/a	*s/n* ratio for IL-2	n/a
s/n ratio for TNF-α	3326.92	*s/n* ratio for TNF-α	20.00
SEB-Stimulated CD4⁺ stained for IL-13	***s/n* ratio**	**SEB-Stimulated CD8⁺ stained for IL-13**	***s/n* ratio**
s/n ratio for CD40L	1.39	*s/n* ratio for CD40L	n/a
s/n ratio for IFN-γ	0.57	*s/n* ratio for IFN-γ	n/a
s/n ratio for IL-2	29.90	*s/n* ratio for IL-2	n/a
s/n ratio for TNF-α	59.81	*s/n* ratio for TNF-α	23.92
SEB-Stimulated CD4⁺ stained for IL-2	***s/n* ratio**	**SEB-Stimulated CD8⁺ stained for IL-2**	***s/n* ratio**
s/n ratio for CD40L	91.34	*s/n* ratio for CD40L	122.22
s/n ratio for IFN-γ	55.64	*s/n* ratio for IFN-γ	305.13
s/n ratio for IL-13	5666.67	*s/n* ratio for IL-13	152.78
s/n ratio for TNF-α	1304.90	*s/n* ratio for TNF-α	26.54
SEB-Stimulated CD4⁺ stained for TNF-α	***s/n* ratio**	**SEB-Stimulated CD8⁺ stained for TNF-α**	***s/n* ratio**
s/n ratio for CD40L	599.08	*s/n* ratio for CD40L	134.15
s/n ratio for IFN-γ	209.20	*s/n* ratio for IFN-γ	n/a
s/n ratio for IL-13	4798.17	*s/n* ratio for IL-13	n/a
s/n ratio for IL-2	n/a	*s/n* ratio for IL-2	n/a

7.4.5. Linearity

Considering both $CD4^+$ and $CD8^+$ populations, the assay is demonstrated to produce linear results except for IL-13 cytokine. For the latter, it was not possible to narrow the range of dilutions for linearity evaluation as the number of positive cells for this cytokine obtained in the undiluted SEB-stimulated samples was too low.

Linearity curves for $CD4^+$ and $CD8^+$ populations are showed in Figures 15 and 16, respectively.

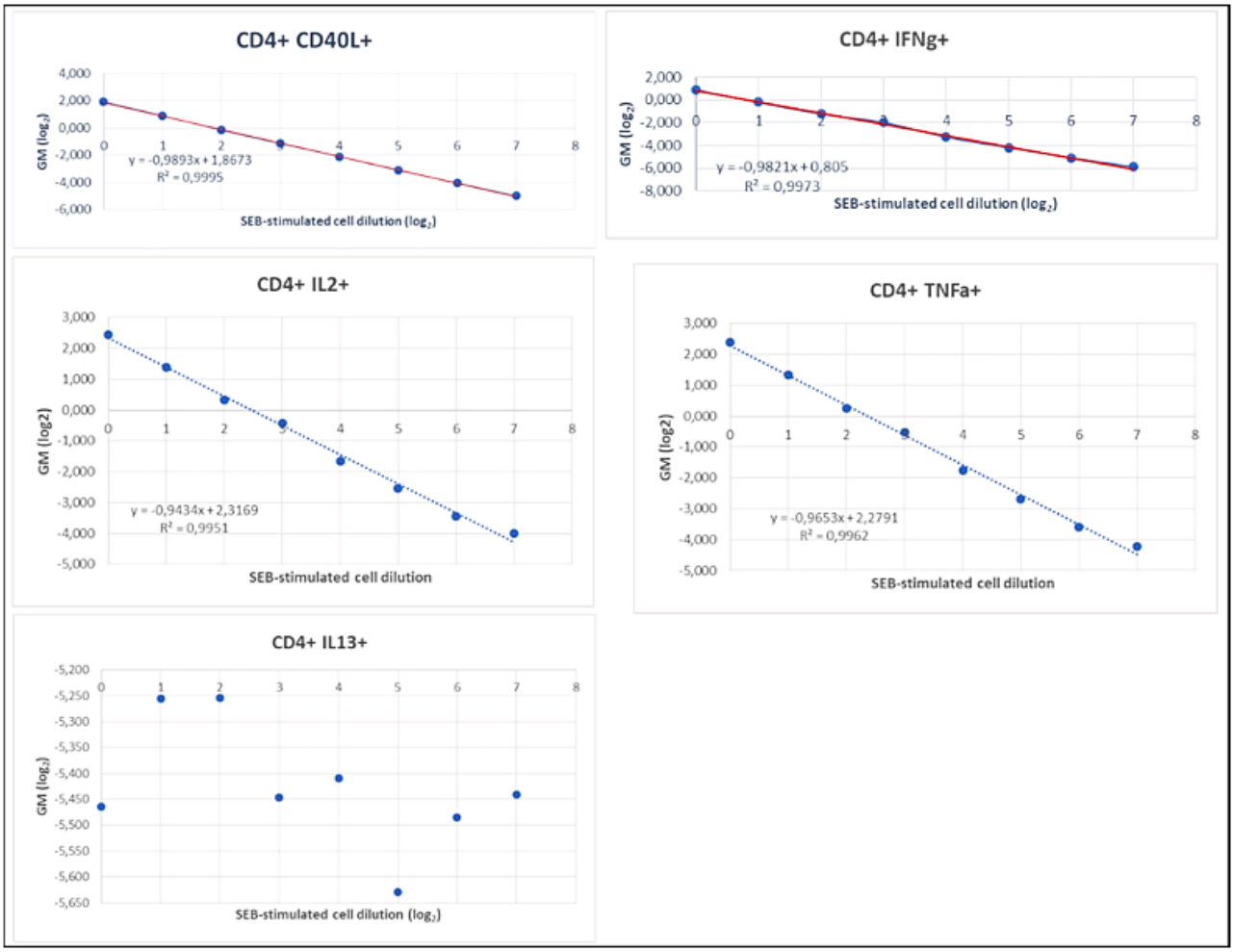

Figure 15: $CD4^+$ population linearity curves. For $CD40L^+$, IFN-γ^+, $IL2^+$, TNF-α^+ the assay demonstrates to produce linear results, while for $IL13^+$ it was not possible to evaluate linearity as the number of positive cells obtained in the undiluted SEB-stimulated samples was too low.

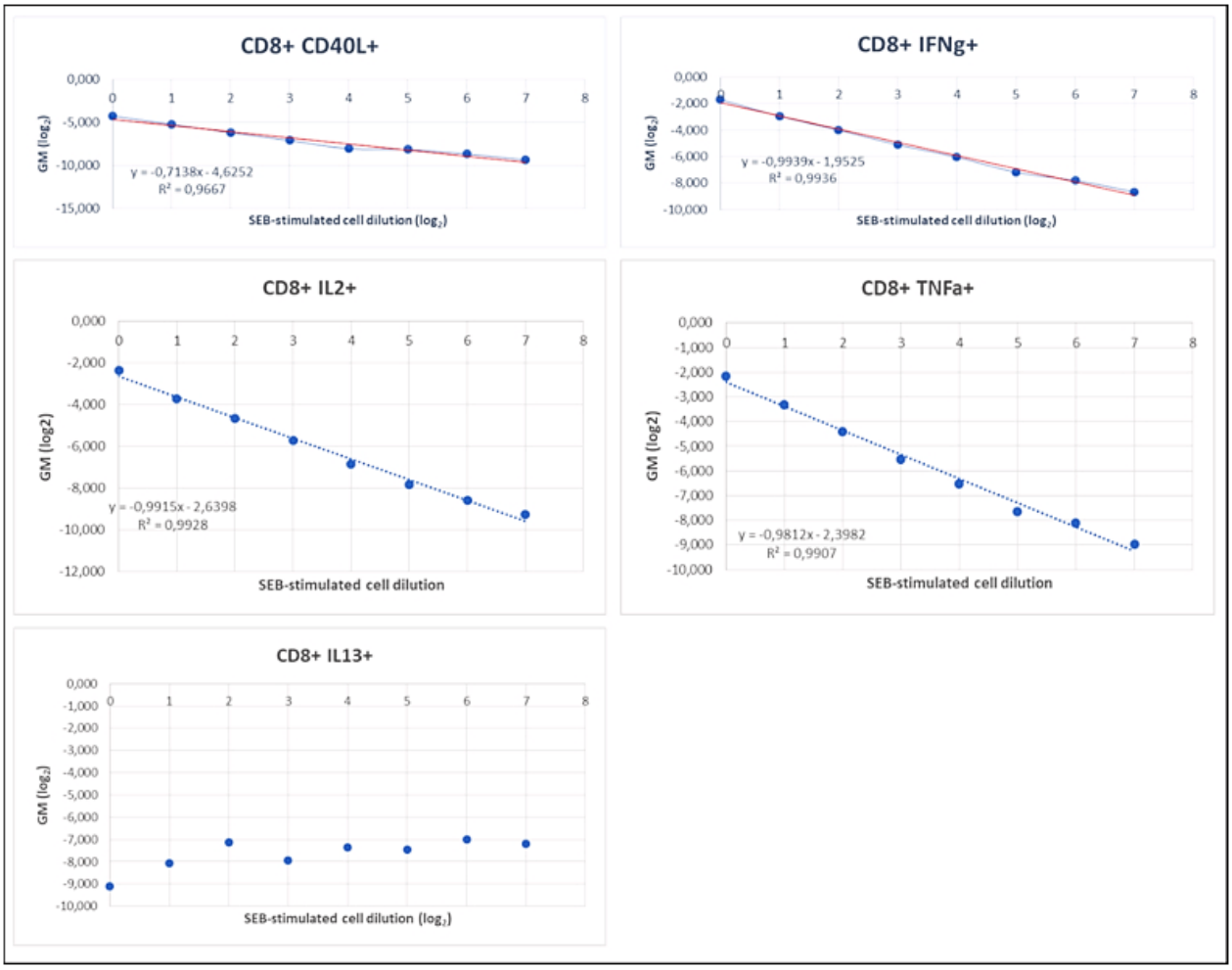

Figure 16: $CD8^+$ population linearity curves. For $CD40L^+$, IFN-γ^+, $IL2^+$, TNF-α^+ the assay demonstrates to produce linear results, while for $IL13^+$ it was not possible to evaluate linearity as the number of positive cells obtained in the undiluted SEB-stimulated samples was too low.

7.4.6. Relative accuracy

Concerning $CD4^+$ population, the assay met the acceptance criteria for relative accuracy for all the cytokines evaluated at all the dilutions tested with the exception of IL-13 for all dilutions tested (1:2 to 1:128) and the highest dilution tested (1:128) for IL-2 and TNF-α (Table 6).

For $CD8^+$ population, only a few dilutions tested for some of the cytokines met the acceptance criteria for relative accuracy. The acceptance criteria were not met for CD40L from 1:32 to 1:128 dilutions, for INF-γ from 1:8 to 1:32 dilutions, for IL-13 from 1:2 to 1:128 dilutions (all dilutions tested), for IL-2 for 1:2 and from 1:8 to 1:32 dilutions and for TNF-α from 1:8 to 1:32 dilutions (Table 7).

Table 6: Relative accuracy results for $CD4^+$ population.

Cytokine	Fold Dilution	Relative Accuracy

		%
CD40L	1	100%
	2	98%
	4	92%
	8	93%
	16	97%
	32	95%
	64	101%
	128	105%
IFN-γ	1	100%
	2	92%
	4	91%
	8	109%
	16	88%
	32	92%
	64	98%
	128	114%
IL-13	1	100%
	2	231%
	4	463%
	8	810%
	16	1662%
	32	2855%
	64	6311%
	128	13011%
IL-2	1	100%
	2	96%
	4	93%
	8	109%
	16	93%
	32	101%
	64	108%
	128	146%
TNF-α	1	100%
	2	97%
	4	91%
	8	107%
	16	91%
	32	95%
	64	101%
	128	130%

Table 7: Relative accuracy results for $CD8^+$ population.

Cytokine	Fold Dilution	Relative Accuracy %
CD40L	1	100%

	2	101%
	4	104%
	8	110%
	16	114%
	32	211%
	64	296%
	128	368%
IFN-γ	1	100%
	2	83%
	4	80%
	8	75%
	16	78%
	32	71%
	64	92%
	128	103%
IL-13	1	100%
	2	414%
	4	1567%
	8	1809%
	16	5351%
	32	10135%
	64	27410%
	128	48382%
IL-2	1	100%
	2	79%
	4	82%
	8	80%
	16	72%
	32	72%
	64	87%
	128	108%
TNF-α	1	100%
	2	89%
	4	84%
	8	77%
	16	78%
	32	71%
	64	103%
	128	113%

7.5. Discussion

All the results obtained in this validation study fulfilled the acceptance criteria evaluated except for IL-13 cytokine in both $CD4^+$ and $CD8^+$ populations, for which specific considerations have been made in paragraph 6.4.1.

From the analysis of the undiluted SEB-stimulated $CD8^+$ IL-13 cells, it has been observed that the mean value calculated was below the 99% confidence interval of the LOD estimated over the undiluted unstimulated $CD8^+$ IL-13 cells. Since the expected value for IL-13 in both $CD4^+$ and $CD8^+$ populations was below the threshold of the LOD distribution it was not possible to reliably distinguish the results of SEB-stimulated cells from the results of the unstimulated cells. The failure to detect IL-13 expressing cells was not due to an incorrect choice of the dilution for IL-13 antibody used for the present validation study, and for testing of the clinical trial samples, as the optimal dilution of antibody to detect IL-13 on $CD4^+$ and $CD8^+$ cells was selected based on the MFI.

The main reason the $CD8^+$ subpopulation failed to meet the relative accuracy acceptance criteria was the extremely low values of $CD8^+$ cells positive for the cytokines evaluated, even in the undiluted SEB-stimulated sample. In fact, even though it is reported in literature that IL-13 is secreted not only by T helper cells, but also by $CD8^+$ T cells following activation, it was possible that the low IL-13 production observed during these experiments could be related to its main role in the pathogenesis of IgE-mediated allergic diseases and not specifically in response to antigens [83]. Hence, the poor relative accuracy was not an inherent property of the flow cytometry assay rather it was a consequence of trying to measure a rare event.

The evaluation of cell mediated immunity through multicolour flow cytometry can provide further information regarding the development of immunity induced by a vaccine as well as for the follow up of patients in clinical trials. In most cases, the evaluation of vaccine immunogenicity is performed by using serological assays. However, considering the complexity of the immune response and that new vaccines may produce low levels of antibody response, serological evaluation cannot be sufficient to determine the effectiveness of a vaccine. For this reason, cell-mediated immune response upon a vaccination is increasingly being investigated, although currently it represents an exploratory endpoint since no correlates of protection regarding either the phenotype or the magnitude of the immune cell response following vaccination have yet been established [71, 84, 85].

Several studies have been performed with the aim to harmonize experimental steps of such technique as well as gating approach [86] in order to reduce the variability across laboratories. With the scope to obtain solid evidence regarding the suitability of flow cytometry as tool for the evaluation of clinical samples and immune monitoring, the

method, and thus also reagents used, has to be validated [87]. The present validation approach has been developed in order to demonstrate the suitability of the assay for its following use to process clinical samples derived from clinical trials; unfortunately, the unavailability of different human PBMCs donor samples did not allow the evaluation of robustness criteria, representing a limit of the present study.

In conclusion, it has been demonstrated that the assay was able to detect and quantify IL-2, CD40L, IFN-γ and TNF-α cell markers in specific live $CD4^+$ and $CD8^+$ cell populations and it could be used for the assessment of the immune response in clinical samples from epidemiology studies and vaccine clinical trials after stimulation with stimulating agents. Concerning IL-13 cytokine, it has been established that for the evaluation of clinical samples it would have been measured as positive (when above the LOD) or negative (when at or below the LOD).

8. TASK 2

8.1. Introduction

Generally, symptomatic treatment for Influenza is reserved to people not belonging to high-risk groups showing symptoms such as fever, colds, cough; on the contrary, people belonging to high-risk group should be promptly treated with antivirals in addition to symptomatic therapy. Therefore, an early diagnosis for Influenza infection is meaningful to allow timely treatment and increase the implementation of public health measures.

A definitive diagnosis can be made by having an appropriate collection of respiratory samples and with the application of a rapid laboratory test. In this regard, the molecular identification of Influenza through Real-time Reverse Transcription Polymerase Chain Reaction (Real-time RT-PCR) is a rapid and sensitive assay for the detection, characterization and quantization of influenza viruses [88].

8.2. Real-time RT-PCR

The Real-time RT-PCR is a technique that combine the reverse transcription of RNA into complementary DNA (cDNA) and amplification of specific DNA targets by using the polymerase chain reaction [89]. This process allows to amplify a single molecule into millions of copies in short times. The amplification is achieved by three different steps, which make up a complete cycle [90-92]:

1. Denaturation: double-stranded DNA templates are heated in order to separate the strands by breaking the hydrogen bonds between the nucleotide base pairs. This step usually occurs at 94-98°C, depending on the specific polymerase involved and it can take up to 2 minutes to complete the denaturation.

2. Annealing: in this step two short oligonucleotides called primers (synthetic short DNA strand) anneal at complementary sequences of the denaturated DNA strands. The annealing temperature has a key role at this stage, it should be 5°C below the lowest melting temperature of both primers. Usually the temperature ranges between 52-58°C in a time of 15-60 seconds.

3. Extension: at this point the polymerase activity of binding nucleotides to the annealed primer leads to an exponential amplification of the template strand. Generally, this step can be carried out at 70-80°C for 1-2 minutes, depending on the polymerase nature. The resulting amplicon can then be visualized through staining with dye or through labelling with fluorescent nucleotides or primers.

Real-time RT-PCR can be executed by using different step methods. The one applied for this validation study is the one-step method. In this way the reagents for retro-transcription and PCR are added to the same tube allowing both reactions to occur simultaneously. The advantages are the reduced times, the lower probability of contamination and the higher reproducibility considering less pipetting [93].

Real-time RT-PCR instruments show an amplification curve (logarithmic or exponential) that can be divided in three phases: the initiation phase, the exponential phase and the plateau (Figure 17).

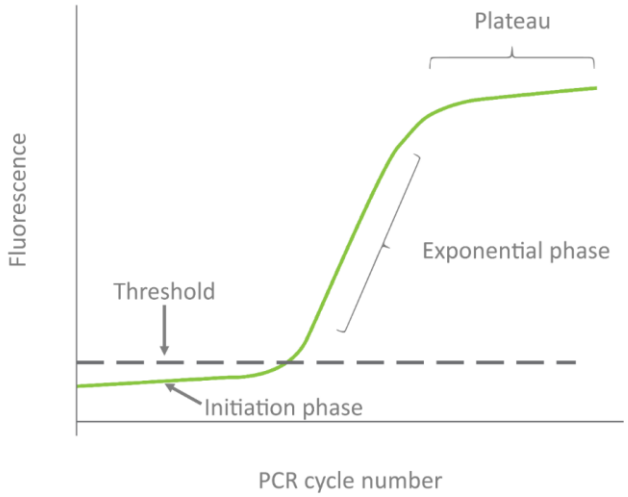

Figure 17: Real-time RT-PCR amplification phases. The initiation phase occurs during the first PCR cycles, in which the fluorescence cannot be distinguished from the baseline. During the exponential phase there is an exponential increase in fluorescence signal until plateau phase is reached. In this last phase of the process, reagents are exhausted and no increase in fluorescence signal is reported.

In the initiation phase very low levels of fluorescence are detected because a very small amount of amplicon has been produced. The threshold value is the level at which fluorescence reaches values above the baseline, it can be set manually or automatically by the analysis software. In the exponential stage the subsequent cycles of amplification lead to an exponential increase of copies of target DNA, demonstrated by an increase of fluorescence. In the last phase, the plateau, amplification is no longer occurring

exponentially due to the exhaustion of reagents and, therefore, fluorescence signal is not detected [91, 92].

The need to analyse targets in real-time has led to the emergence of novel fluorescent DNA labelling techniques. One of them, and the one chosen for the present study, is the TaqMan technology (Figure 18).

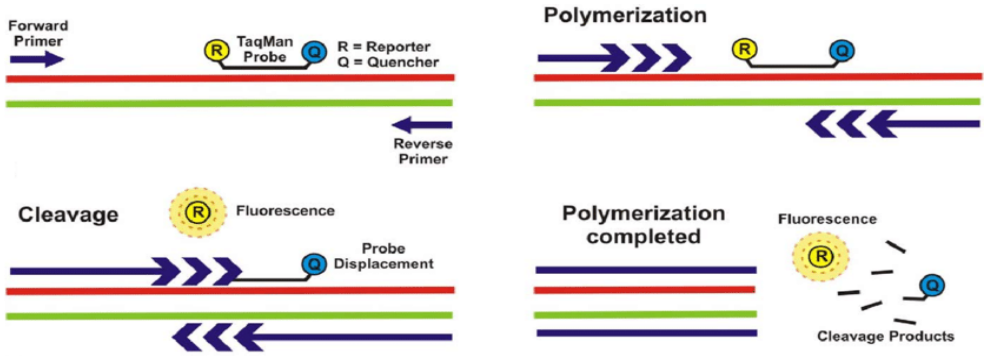

Figure 18: TaqMan technology. TaqMan probe has a reporter (fluorophore) at 5'-end and a quencher at 3'-end that inhibit the fluorescence signal. During the polymerization, Taq polymerase degrades the annealed probe to the template. In the cleavage phase, the reporter is removed from the quencher showing a fluorescence signal.

TaqMan probes are generated by a fluorophore covalently attached to the 5'-end of the oligonucleotide probe and by a quencher at the 3'-end. The quencher molecule quenches the fluorescence emitted by the fluorophore when excited by the instrument light source; as long as the quencher is near to the fluorophore, the fluoresce signal is inhibited. When the Taq polymerase extends the primer and synthetize the new strand, its 5' to 3' exonuclease activity degrades the probe that has annealed to the template. In this way, the fluorophore is released and removed from the quencher molecule allowing to emit a fluorescence signal that can be detected by the instrument. The detected fluorescence is directly proportional to the fluorophore released and to the amount of target present in the PCR [94].

8.3. Materials and method

8.3.1. Influenza strains

Influenza strains tested and assigned abbreviations are listed in Table 8. Six Influenza viruses A and six Influenza viruses B reference strains were used to evaluate the method.

Table 8: List of Influenza strains tested during Real-time RT-PCR validation experiments.

Strain	Abbreviation
A/Singapore/GP1908/2015 IVR-180 (H1N1) cell-derived cell	A/Sing

grown	
A/Brisbane/10/2010 (H1N1) cell-derived cell grown	A/Bris
A/Idaho/07/2018 (H1N1) cell-derived cell grown	A/Idaho
A/Indiana/08/2018 (H3N2) cell-derived cell grown	A/Ind
A/North Carolina/04/2016 (H3N2) cell-derived cell grown	A/North
A/Hong Kong/4801/2014 (H3N2) cell-derived cell-grown	A/HK
B/Iowa/06/2017 (Victoria Lineage) cell-derived cell grown	B/Iowa
B/Brisbane/60/2008 (Victoria Lineage) cell-derived cell grown	B/Bris
B/Colorado/06/2017 (Victoria Lineage) cell-derived cell grown	B/Colo
B/Massachusetts/02/2012 (Yamagata Lineage) egg-derived cell-grown	B/Mass
B/Singapore/INFTT-16-0610/2016 (Yamagata Lineage) cell-derived cell grown	B/Singa
B/Utah/09/2014 (Yamagata Lineage) cell-derived cell grown	B/Utah

8.3.2. Viral RNA extraction and purification

Viral RNA was extracted by using the commercial extraction kit "QIAmp Viral RNA Mini Kit" (Qiagen) as described below.

One part of buffer AVE containing RNA-carrier was added to 100 parts of buffer AVL and the solution was gently mixed by inverting the tube. One part of sample was added to 4 parts of buffer AVL containing the solution buffer AVE-RNA carrier; the resulting solution was mixed by pulse-vortexing for 15 seconds and incubated for 10 min at RT. The tube was briefly centrifuged to remove drops from the inside of the lid. Ethanol (96-100%) was added to the resulting solution and the mixture was then mixed by pulse-vortexing. The first half of the resulting solution was applied to the QIAmp Mini Column and adjusted into a new 2.0 ml collection tube. Samples were centrifuged at 6000 g for 1 min (fixed angle rotor, RPM 8069, radius 8.23 cm, $RCF = 11.2 \times Radius \times (RPM/1000)^2$) and the flow through was discarded; this step was repeated twice. Buffer AW1 was added to the column, samples were centrifuged at 6000 g for 1 min and the flow through was discarded. Buffer AW2 was added to the column, samples were centrifuged at 16000 g for 3 min (fixed angle rotor, RPM 13180, radius 8.23 cm, $RCF = 11.2 \times Radius \times (RPM/1000)^2$) and the flow through was discarded. The column was then applied into a new collection tube and buffer AVE was added, samples were centrifuged at 6000 g for 1 min.

8.3.3. One-step Real-time RT-PCR

In order to characterize Influenza viruses, purified viral RNA was tested by primers/probe sets selected from highly conserved regions of the matrix protein (M) gene of Influenza virus A and the hemagglutinin (HA) gene segment of Influenza virus B and highly conserved regions of the HA gene segment for related subtypes [95]. Oligonucleotides were designed following WHO guidelines [88] as listed in Table 9.

Table 9: List of Influenza strains tested during Real-time RT-PCR validation experiments.

Virus (Target)	**Oligonucleotide**	**Sequence**
Influenza B virus *HA* gene	Forward primer	AAATACGGTGGATTAAACAAAAGCAA
	Reverse primer	CCAGCAATAGCTCCGAAGAAA
	Probe	**Fam-** CACCCATATTGGGCAATTTCCTATGGC-**QSY**
Influenza A virus *M* gene	Forward primer	CTTCTAACCGAGGTCGAAACGTA
	Reverse primer	GGTGACAGGATTGGTCTTGTCTTTA
	Probe	**VIC-**TCAGGCCCCCTCAAAGCCGAG-**QSY**
A(H1)pdm09 *HA* gene	Forward primer	AAACTATGCAAACTAAGAGGGGT
	Reverse primer	TGTTTCCACAATGTAGGACCA
	Probe	**VIC-**CCAGAGTGTGAATCACTCTCCACA-**QSY**
A (H3) *HA* gene	Forward primer	ACCCTCAGTGTGATGGCTTTCAAA
	Reverse primer	TAAGGGAGGCATAATCCGGCACAT
	Probe	**Fam-** ACGAAGCAAAGCCTACAGCAACTGTT-**QSY**
A (H3) *HA* gene	Forward primer	GCACAGGGAATCTAATTGCTCC
	Reverse primer	ATGCTTCCATTTGGAGTGATGCATTC
	Probe	**Fam-**

		GATCAGATGCACCCATTGGCAAATGC-**QSY**
B *HA* gene	Forward primer	AGACCAGAGGGAAACTATGCCC
B *HA* gene	Reverse primer	TCCGGATGTAACAGGTCTGACTT
B (Victoria lineage)	Probe	**VIC-**CAGACCAAAATGCAC**G**GGGAAAATACC-**QSY**
B (Yamagata lineage)	Probe	**Fam-**CAGGCCAATGTGTGTGGGGA*C*CACACC-**QSY**

The applied reaction was a duplex, allowing the simultaneous detection of two different targets with no cross-reaction. The first screening was to distinguish Influenza virus A and Influenza virus B. A further one allowed to distinguish subtype H1pdm09 and H3N2 of Influenza virus A and lineage B/Victoria and B/Yamagata of Influenza virus B. Reference strains listed in Table 8 were tested by using a duplex Real-time RT-PCR technique: Influenza A *vs* B, H1pdm09 *vs* H3N2 subtype and B/Victoria *vs* B/Yamagata lineage.

Duplex master mixture was prepared by using TaqMan® Fast Virus 1-Step Master Mix, two different forward primers and two different reverse primers at final concentration of 900 nanomolar (nM) each, two different fluorogenic probes at final concentration of 250 nM and nuclease-free sterile water. The master mixture was centrifuged for 5 seconds, placed in a cold rack and then seeded into each well across the test plate. RNA samples were seeded into each well of the test plate and analysis was acquired by the instrument (Applied Biosystems QuantStudio 5 interfaced to PC QuantStudio™ Design & Analysis Software v 1.5.1). All the reagents and the instrument listed above were purchase from Thermo Fisher. Specific setting was applied, as shown in Table 10.

Table 10: Instrument settings.

Step	Temperature (C°)	Time
Reverse Transcription	50	20 min
Initial PCR activation	95	5 min

PCR amplification	45 cycles	
Denaturation	95	15 sec
Annealing/extension	60	45 sec

Each sample was composed of purified RNA from two separate reference viruses which were analyzed in the same well as a duplex and tested in eight different analytical tests (two operators for four independent days) with three replicates' measurements per sample dilution. Two different conditions were investigated in order to demonstrate that the method was not affected by external changes. In the same plate, purified RNA from reference viruses was seeded (one single repetition) as the negative and specificity control for the targets of interest [96]. In addition, Negative Template control (NTC) sample treated as all tested samples was eluted following RNA extraction and purification protocol from a sample of nuclease-free sterile water.

8.4. Validation parameters

The assay validation criteria were selected from the ICH and FDA guidelines.

Sensitivity and limit of detection (LOD)

The sensitivity of a Real Time RT-PCR method can be expressed as the LOD. The LOD value is calculated from blank samples in the validation analysis. It is expressed in threshold cycle (Ct) value which is determined by the arithmetic mean of all blank samples subtracted with 3.3 times the standard deviation of blank samples. Blank samples are represented by NTC samples and negative controls (unrelated influenza virus strains) measured across conditions, days and operators.

The applied formula was: *LOD= Mean (blank) - 3.3*Standard Deviation (SD) (blank)*.

Linearity

Viral RNA extracted from stock Influenza viruses were 10-fold diluted for 7 steps. Three replicates of each sample were tested. Test was repeated in four independent days by two operators.

Geometric mean of Ct (GMCt) within the tests was calculated between replicates for each viral strain, for each operator, for every day, for every reaction condition. If NTC and negative controls resulted as “Undetermined”, these were arbitrary considered with Ct=40.0 [88].

The assay was considered to have acceptable linearity if for the virus strain, the coefficient of determination R^2 of the linear model is ≥ 0.98, and the slope was between -3.6 and -3.1 reflecting an efficiency of 100%±10%.

Amplification efficiency

Linearity results were used to evaluate the amplification efficiency by using the slope of the regression line. The applied formula for the Real-time RT-PCR efficiency (ε) was: $\varepsilon = 100 \cdot (10^{-1/slope} - 1)$.

The amplification efficiency was considered acceptable between 90% and 110%.

Relative accuracy

Relative accuracy was assessed as the agreement between the expected and observed GMCt across the dilution series.

The assay was considered to have acceptable relative accuracy for all samples where the observed GMCt of all replicates for each strain was within 80% to 120% of the expected value.

Precision – Repeatability

The repeatability or intra-assay precision was determined per operator, within run.

The Geometric Coefficient of Variation percentage (%GCV) of intra-assay variability for each dilution was considered acceptable with a value ≤20%.

Precision – Intermediate precision

The intermediate Precision or inter-assay precision was determined across two operators across different days.

The Geometric Coefficient of Variation percentage (%GCV) of intra-assay variability for each dilution was considered acceptable with a value ≤20%.

Limits of quantitation and range

The results obtained from the above parameters evaluations were used to determine the limits of quantitation and range of the assay. The range was defined as the interval within which the assay was demonstrated to produce linear, accurate and precise results.

Format variability

The format variability represented the variation expected across GMCt results produced from multiple replicates in routine testing.
The acceptance criterion was set with a %GCV <10%.

Specificity

The specificity parameter was assessed for each test by using specific oligonucleotides for each viral RNA subtype showing signal. Negative and positive controls using specific oligonucleotides mix had to show no amplification signal for unspecific reagents, but amplification signal for the specific ones.

Robustness

The robustness was evaluated by changing standard reaction conditions of annealing temperature. For this evaluation, the temperature was increased by one degree.
This parameter was evaluated in the descriptive variance component analysis to determine whether the reaction condition effect caused a significant contribution to the Ct results. Estimates of the reaction condition fixed ranging between $\log_{10}(0.8)$ and $\log_{10}(1.2)$ indicated an acceptable assessment of robustness. This interval corresponds to a limit of 20% variation between the overall GMCt calculated under the standard condition and the overall GMCt calculated under the annealing-temperature condition.

8.5. Results

8.5.1. Sensitivity and LOD

The LOD determined the Ct interval as the range in which the assay was demonstrated to produce linear, accurate and precise results. LOD was expressed in Ct values which are determined by the arithmetic mean of all blank samples subtracted with 3.3 times the standard deviation of blank samples. Blank samples are represented by NTC samples and

negative controls (unrelated influenza virus strains) measured across conditions, days and operators. Ct intervals for all duplex analyses (H1pdm09 *vs* B/Victoria, H3N2 *vs* B/Yamagata, H1pdm09 *vs* H3N2, B/Victoria *vs* B/Yamagata) are reported in Figure 19.

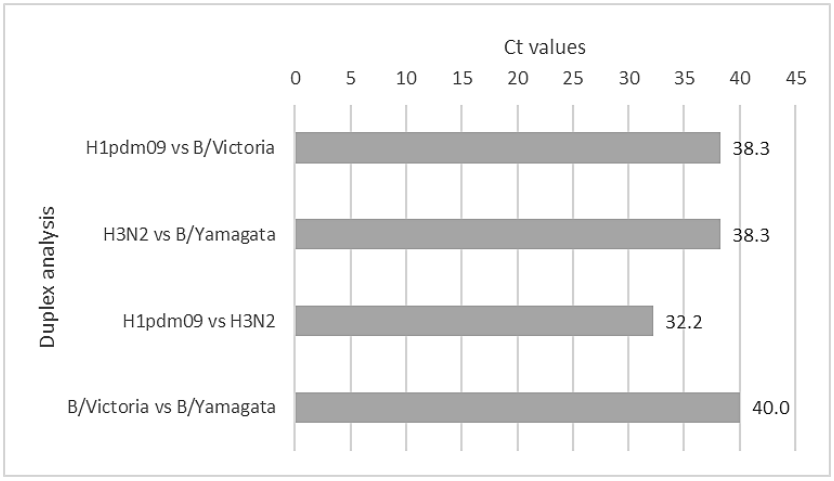

Figure 19: Detection limit graph for each duplex analysis. For H1pdm09 vs B/Victoria duplex analysis the LOD is set as a Ct value of 38.3; for H3N2 vs B/Yamagata analysis as a Ct value of 38.3; for H1pdm09 vs H3N2 analysis as a Ct value of 32.2; for B/Victoria vs B/Yamagata as a Ct value of 40.0.

LOD for H1pdm09 *vs* B/Victoria analysis was set as a Ct value of 38.3; for H3N2 *vs* B/Yamagata analysis as a Ct value of 38.3; for H1pdm09 *vs* H3N2 analysis as a Ct value of 32.2; for B/Victoria *vs* B/Yamagata as a Ct value of 40.0. Ct values higher than 40.0 or reported as “no amplification” by analytical software were considered as “Undetermined” for the targets in exam and arbitrary reported as 40.0.

8.5.2. Linearity

The GMCt within the tests was calculated between replicates for each viral strain, for each operator, for every day, for every reaction condition.

If NTC and negative controls resulted as “Undetermined”, these were considered as Ct=40.0 [88]. Dilution Linearity curves for each duplex analysis using reference viruses were shown to meet the acceptance criteria and are reported in Figure 20.

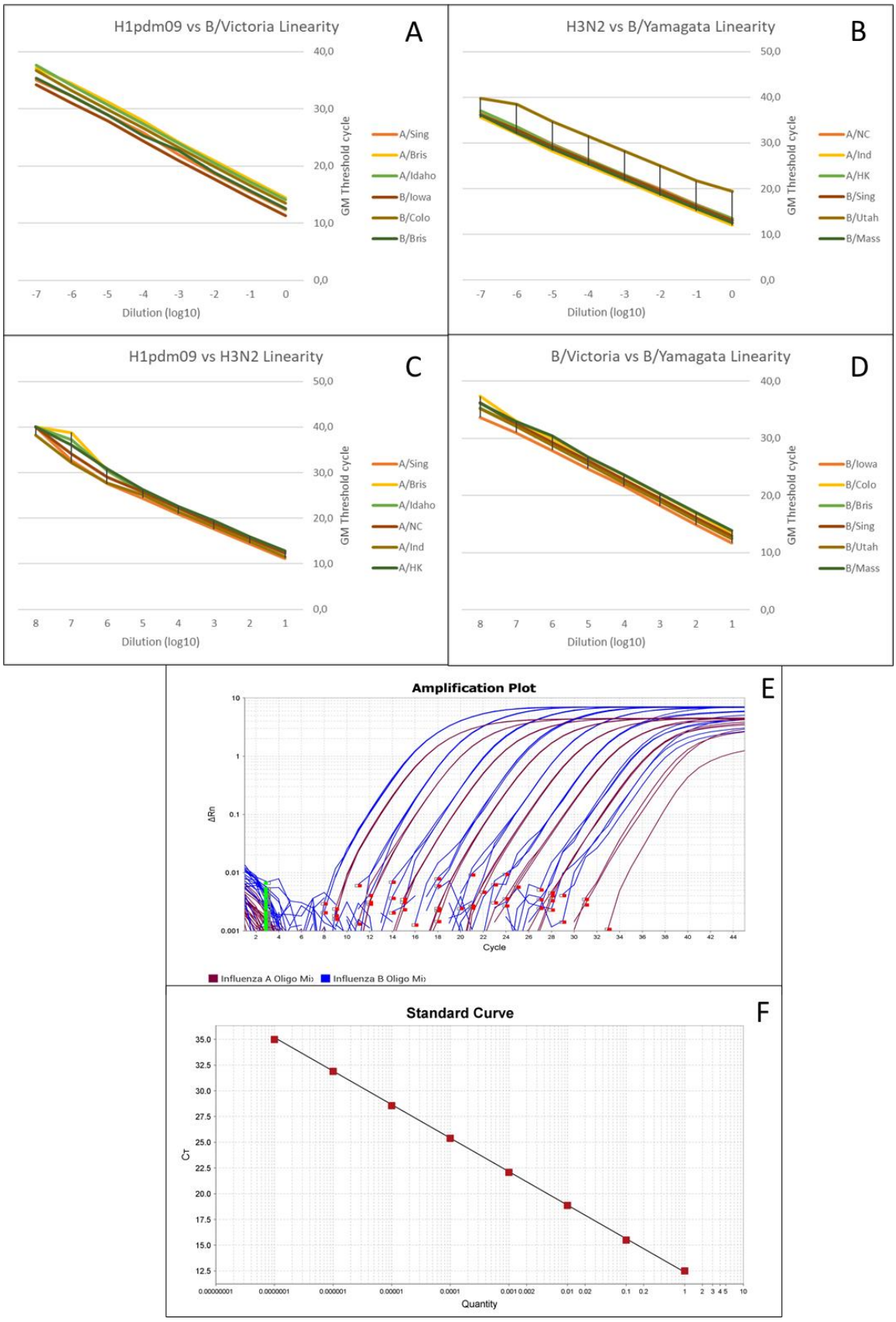

Figure 20: Dilution linearity curves for each duplex analysis using reference viruses (A-D). Example of amplification plot (logarithmic graph type) with curves related to three replicates of reference viruses A and B using duplex reaction (Influenza A and B oligonucleotides mix) from undiluted sample to 1:10^7 diluted one (E). Example of standard curve generated by the analysis software (F).

8.5.3. Amplification efficiency

An efficiency percentage close to 100% is an indicator of a robust and reproducible assay. Considering a 10-fold dilution scheme for the analysed sample, the difference between Ct values of consecutive sample dilutions should be around 3.3, given 100% amplification efficiency. However, there are some factors that can impact the amplification efficiency percentage and Ct values might not shift accordingly: presence of inhibitors of the polymerase enzyme, pipetting errors, inaccurate dilution series, unspecific products. In this case there could be a lower slope and an amplification efficiency over 100%. Therefore, considering the assay variability, values of efficiency between 90% and 110% were considered acceptable. Obtained values for each strain in each duplex analysis are reported in Table 11 (viral strains abbreviations are reported in Table 8).

Table 11: Amplification efficiency results for each strain in each duplex analysis.

H1pdm09 *vs* B/Victoria	
Viral Strain	**Amplification Efficiency (%)**
A/Sing	100.500
A/Bris	100.754
A/Idaho	98.072
B/Iowa	100.838
B/Colo	100.081
B/Bris	102.214
H3N2 *vs* B/Yamagata	
Viral Strain	**Amplification Efficiency (%)**
A/North	99.581
A/Ind	98.233
A/HK	97.038
B/Sing	101.136
B/Utah	109.176
B/Mass	98.923
H1pdm09 *vs* H3N2	

Viral Strain	Amplification Efficiency (%)
A/Sing	93.471
A/Bris	93.070
A/Idaho	93.070
A/North	91.045
A/Ind	97.672
A/HK	91.958
B/Victoria *vs* B/Yamagata	
Viral Strain	**Amplification Efficiency (%)**
B/Iowa	106.519
B/Colo	99.457
B/Bris	100.923
B/Sing	100.290
B/Utah	101.996
B/Mass	105.353

The acceptance criterion was met for each duplex analysis demonstrating that the assay has an amplification efficiency close to 100% on average, which corresponds to obtaining a double number of molecules of the target during each replication cycle.

8.5.4. Relative accuracy

The relative accuracy was evaluated by calculating the percentage of recovery on the GMCt of the reportable Ct values (across conditions, days and operators) and the expected (true) one. For its evaluation, results obtained from linearity assessment were used.

The assay was considered to have acceptable relative accuracy for all samples where the observed GMCt of all replicates obtained for a sample was within 80% to 120% of the expected value. Obtained values for each dilution for each strain in each duplex analysis are reported in Appendix section (Table 1; viral strains abbreviations are reported in Table 8).

The acceptance criterion was met for all the strains in each duplex analysis. An exception needs to be made for B/Utah (1:10^6 and 1:10^7 dilutions) in H3N2 *vs* B/Yamagata analysis and for A/Sing (1:10^6 and 1:10^7 dilutions), A/Bris (1:10^6 and 1:10^7 dilutions), A/Idaho (1:10^6 and 1:10^7 dilutions), A/North (1:10^6 and 1:10^7 dilutions), A/Ind (1:10^7 dilution), A/HK (1:10^6 and 1:10^7 dilutions) in H1pdm09 *vs* H3N2 analysis. For those strains dilutions the relative accuracy calculation is not applicable because the observed GMCt values are higher than the fixed LOD showed in Figure 19.

8.5.5. Precision

The precision was evaluated at three different stages: intra-assay or repeatability, intermediate precision, and format variability.

Results for each dilution for each strain for each duplex analysis for all the three stages are showed in Appendix section (Table 2; viral strains abbreviations are reported in Table 8).

The acceptance criteria for the three precision parameters were fulfilled for all the strains in each duplex analysis. An exception needs to be made for B/Utah (1:10^6 and 1:10^7 dilutions) in H3N2 *vs* B/Yamagata analysis and for A/Sing (1:10^6 and 1:10^7 dilutions), A/Bris (1:10^6 and 1:10^7 dilutions), A/Idaho (1:10^6 and 1:10^7 dilutions), A/North (1:10^6 and 1:10^7 dilutions), A/Ind (1:10^7 dilution), A/HK (1:10^6 and 1:10^7 dilutions) in H1pdm09 *vs* H3N2 analysis. For those strains dilutions the relative accuracy calculation is not applicable because the observed GMCt values are higher than the fixed LOD showed in Figure 18. In addition, format variability criterion was not met for A/Bris (1:10^5 dilution), A/Idaho (1:10^5 dilution), A/Ind (1:10^6 dilution) and A/HK (1:10^5 dilution) in H1pdm09 *vs* H3N2 analysis.

8.5.6. Specificity

Each viral RNA sample was tested in triplicate, showing an amplification signal when using specific oligonucleotides sets.

Ct averages obtained with specific and unspecific reagents for each duplex analysis during specificity evaluation are reported in Table 12.

Table 12: Ct averages for each duplex analysis obtained by using specific and unspecific oligonucleotides sets.

Analysis	Sample	Oligonucleotides Set	Ct Average
A *vs* B duplex (H1pdm09 *vs*	Influenza Virus A	Specific oligonucleotides	19.5
		Unspecific oligonucleotides	39.9

B/Victoria)	Influenza Virus B	Unspecific oligonucleotides	39.9
		Specific oligonucleotides	20.6
A *vs* B duplex (H3N2 *vs* B/Yamagata)	Influenza Virus A	Specific oligonucleotides	19.7
		Unspecific oligonucleotides	40.0
	Influenza Virus B	Unspecific oligonucleotides	39.8
		Specific oligonucleotides	18.8
H1pdm09 *vs* H3N2 duplex	Influenza Virus H1pdm09	Specific oligonucleotides	18.7
		Unspecific oligonucleotides	38.7
	Influenza Virus H3N2	Unspecific oligonucleotides	40.0
		Specific oligonucleotides	18.4
B/Victoria *vs* B/Yamagata duplex	Influenza Virus B/Victoria	Specific oligonucleotides	18.8
		Unspecific oligonucleotides	40.0
	Influenza Virus B/Yamagata	Unspecific oligonucleotides	40.0
		Specific oligonucleotides	19.2

Primers and Probes exploited during the validation study were shown to be specific for all duplex analysis. Indeed, Ct averages for unspecific oligonucleotides are higher than the set LOD.

For A *vs* B duplex analysis (H1pdm09 *vs* B/Victoria) Ct averages for specific oligonucleotides were 19.5 and 20.6, while Ct averages for unspecific oligonucleotides were 39.9.

For A *vs* B duplex analysis (H3N2 vs B/Yamagata) Ct averages for specific oligonucleotides were 19.7 and 18.8, while the ones for unspecific oligonucleotides were 39.8 and 40.0.

For H1pdm09 *vs* H3N2 duplex analysis Ct averages for specific oligonucleotides were 18.7 and 18.4, while the ones for unspecific oligonucleotides were 38.7 and 40.0.

For B/Victoria *vs* B/Yamagata duplex analysis Ct averages for specific oligonucleotides were 18.8 and 19.2, while the ones for unspecific oligonucleotides were higher than 40.0 (reported as 40.0).

8.5.7. Robustness

In order to demonstrate the robustness criterion, the percentage of change between the two applied reaction conditions was calculated. The obtained percentages were considered acceptable (change between the two different reaction conditions less than 20%) and are reported as absolute values in Table 13.

Table 13: Absolute values of the maximum percentages between the two different reaction conditions.

Subtype or Lineage	***Analysis***	***Maximum % change between reaction conditions***
H1pdm09	A vs B	1.919

	H1pdm09 vs H3N2	6.088
H3N2	A vs B	0.301
	H1pdm09 vs H3N2	3.120
B/Victoria	A vs B	2.283
	B/Victoria vs B/Yamagata	1.978
B/Yamagata	A vs B	2.520
	B/Victoria vs B/Yamagata	2.388

Since all the percentages reported fulfils the acceptance criterion, the assay can be considered robust.

8.6. Discussion

Considering the high impact of Influenza disease on the society it is very important to have a highly sensitive and fast assay that can give an estimation of the vaccine efficacy. RT-PCR assay is a good method for the detection and characterization of Influenza viruses, that can be applied for improving the sanitary surveillance and diagnosing the disease [97].

However, before its application in clinical trials, the assay needs to be validated in order to demonstrate that it met the acceptance criteria for each parameter as requested by the regulatory agency. The aim of this study is to show an approach for the validation of RT-PCR assay by using customized oligonucleotides. Despite the presence of commercially available oligonucleotides kits, the usage of customized ones can allow to increase the specificity in detecting viral subtypes, often not possible with kits. In addition, customized assays can be more specific and more sensitive than currently available antigen detection tests [98]. One of the advantages of this validation study is precisely the usage of oligonucleotides selected from highly conserved regions of the genes for Influenza A and B, making the assay completely validated for all relevant Influenza strains. This is an important aspect for new vaccine efficacy studies in subsequent seasons.

9. TASK 3

9.1. Introduction

The RSV is responsible for the majority of acute lower respiratory tract infections in infants and older adults worldwide. Owing to its widespread infection, the WHO considers it a target for the development of preventive vaccines. Despite the high impact of its infections, however, only two vaccine candidates have been recently approved.

The importance of nAb has been demonstrated by many studies and supported by the evidence that high levels of nAb correlate significantly with protection against RSV disease in adult volunteers. In this regard, the virus microneutralization (MN) assay is a serological method that can detect the presence of functional nAb able to inhibit the virus replication [68].

The present study aimed to document the results obtained during the set-up and validation experiments of the MN assay against RSV-A and B in accordance with the ICH guidelines. The objective is to demonstrate the suitability of this assay for the detection and quantization of serum-nAb, with a view to testing clinical samples in trials evaluating the immunogenicity of new vaccines [40].

9.1.1. MN assay

The MN assay is a sensitive and suitable assay for the detection and quantization of nAb [68]. One of the advantages of this method is that it can detect nAb even at very low concentrations, allowing good discrimination between pre and post vaccination results [99].

There are different ways for the results readout, the one applied for the present study is a faster neutralization assay combined with an ELISA assay (Figure 21).

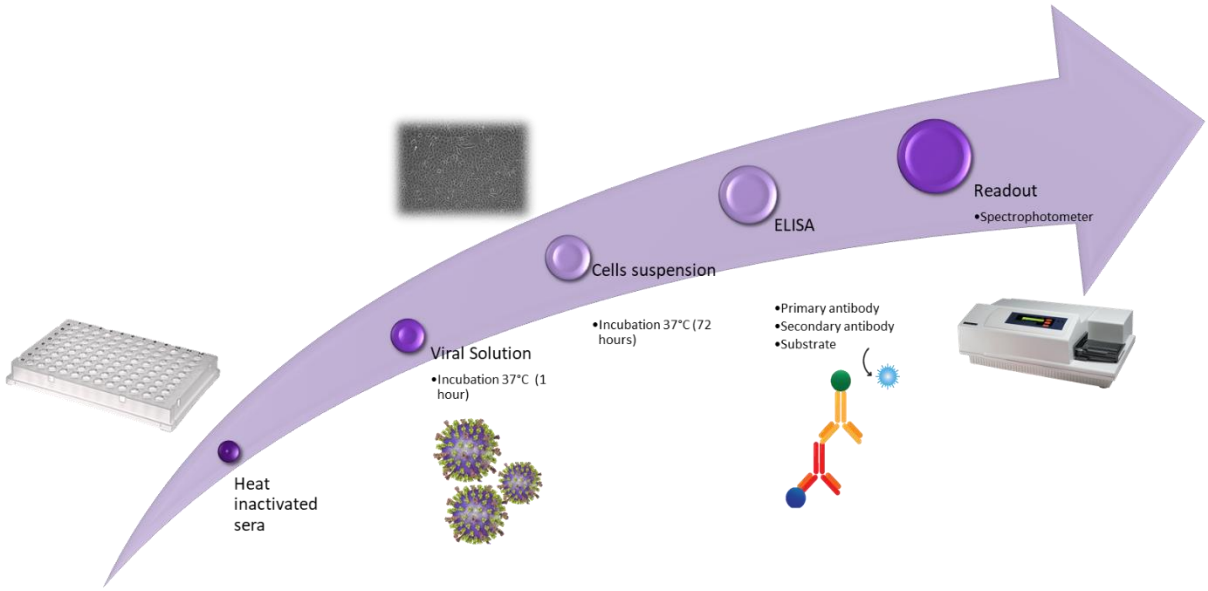

Figure 21: Microneutralization ELISA-based assay scheme. Serum samples are heat inactivated before to be tested and seeded in a 96-well plate with a mixture of viral solution and cells suspension. After 72-hour incubation, primary antibody and then secondary antibody are added. The secondary antibody is conjugated with a molecule that can react with a substrate generating a colorimetric reaction. This reaction generates products that have an absorbance that is detected by the spectrophotometer.

The assay consists of a 72-hour incubation of a mixture of serum samples, virus solution and cells suspension in a 96-wells plate. After the incubation time, plates are blocked, and a primary antibody is added. The primary antibody recognizes and binds the epitope or the specific amino-acid sequence of the protein of interest. A secondary antibody is then added, binding directly on the IgG domain of the primary antibody. The secondary antibody can be conjugated to a fluorophore, enzyme or protein and its scope is to amplify the signal of the primary antibody. The conjugated molecule can react with a substrate generating a colorimetric reaction. This reaction generates soluble products that have an absorbance that can be detected by an instrument, a spectrophotometer.

Results are reported as optical density values by the instrument software and then converted in neutralizing titers.

9.2. Materials and method

9.2.1. Cell culture

Vero cells (American Type Culture Collection [ATCC] #CCL-81) were cultured in Minimum Essential Medium with Earle's salts (EMEM) (Euroclone) supplemented with 10% v/v Fetal Bovine Serum (FBS) (Euroclone), 2 mM L-glutamine, 100 units/mL penicillin, 100 µg/mL

streptomycin (P/S) (Gibco, Life Technologies) with the addition of 1% v/v MEM Non-Essential Amino Acids Solution 100X (Gibco, Life Technologies).

9.2.2. Virus propagation

HEp-2 cells (American Type Culture Collection [ATCC] #CCL-23) were cultured in high-glucose Dulbecco's Modified Eagle's Medium (DMEM) (Euroclone) supplemented with 10% v/v FBS (Euroclone), 2 mM L-Glutamine, 100 units/mL penicillin, and 100 µg/mL Streptomycin (P/S) (Gibco, Life Technologies). Cells were maintained at 37°C, in a humified 5% CO_2 environment, and passaged every 3-4 days.

Human RSV-B WV/14617/85 and human RSV-A were purchased from the American Type Culture Collection (ATCC Number: VR-1400TM and ATCC Number: 1540TM, respectively). Viral propagation was performed in 175 cm^2 tissue-culture flasks pre-seeded with 50 mL of HEp-2 cells (1.0 $x10^6$ cells/mL) diluted in DMEM 10% FBS. After 18-24 hours' incubation at 37°C in 5% CO_2, flasks were washed twice with sterile Dulbecco's phosphate buffered saline w/o Calcium w/o Magnesium (DPBS) (Euroclone) and then inoculated with the RSV-A and B viruses at a multiplicity of infection (MOI) of 0.003. The sub-confluent cell monolayer was incubated with the virus for 2 hours at 37°C in 5% CO_2; flasks were then filled with 50 mL of DMEM 2% FBS and incubated at 37°C in 5% CO_2. Cells were monitored daily until 20-30% of cytopathic effect (CPE) and 60-70% of syncytial formation were observed. The supernatant was removed from the flasks and collected, the cells were scraped, pooled with the supernatant, and centrifuged at 469 g for 5 minutes (rotor A-4-81, RPM 1559, radius 17.3 cm, $RCF = 11.2 \times Radius \times (RPM/1000)^2$) at 4°C to separate the cells from the viral solution. The supernatant was collected, the cell pellet was resuspended in 1 mL of the supernatant, and three freeze-thaw cycles were performed by placing the vial with the cell pellet on ice; the vial was then placed in a 37°C water bath and vortexed (all steps were carried out for 30 seconds). The supernatant previously collected was added to the cell pellet, mixed gently, aliquoted and stored at -80°C in the presence of sucrose.

9.2.3. Serum samples

The experimental set-up for the validation of the Micro-neutralization ELISA-based assay used the commercially available human and animal serum samples reported in Table 14. The antiserum to Respiratory Syncytial Virus WHO 1st International Standard (NIBSC) was used

as a homologous control sample for Specificity experiments, and sheep antisera to Influenza Anti-A/Michigan/45/2015 (H1N1) (NIBSC), Anti-A/Hong Kong/4801/2014 (H3N2) (NIBSC) and Anti-B/Brisbane/60/2008 (B/Victoria) (NIBSC) as heterologous samples. A pool of normal human sera purchased from Discovery Life Sciences was used as a positive sample for Dilutional Linearity experiments. Finally, depleted human serum lacking IgA/IgG/IgM (Sigma-Aldrich) was used as a negative control.

Table 14: Serum samples and controls used in the study.

Positive control	Antiserum to Respiratory Syncytial Virus WHO 1st International Standard (NIBSC) (HS)
Negative control	Negative human serum, Minus IgA/IgM/IgG
Pool of homologous sera	Normal serum, Discovery Life Sciences (cod. 150335)
Heterologous sera	Influenza Anti-A/Michigan/45/2015 (H1N1) (NIBSC) product code 17/106 (HET 1)
	Influenza Anti-A/Hong Kong/4801/2014 (H3N2) (NIBSC) product code 16/182 (HET 2)
	Influenza Anti-B/Brisbane/60/2008 (B/Victoria) (NIBSC) product code 16/192 (HET 3)

9.2.4. Live-Virus Microneutralization ELISA-based assay

The MN assay was performed in 96-well, flat-bottomed, tissue culture, microtiter plates. Homologous and heterologous serum samples (human serum samples had been previously heat inactivated at 56°C for 30 min) were placed in the first well of the microtiter plates at a final concentration of 1:20, and serial two-fold dilutions were performed. All dilutions were performed in MEM medium (Euroclone) with 2% FBS, and the final volume was 50 µL per well. 100 TCID50 (50% tissue culture infectious dose) of virus in 50 µL of MEM with 2% FBS was then added to each well, and the mixture was incubated for 1 h at 37°C in a humidified CO_2 incubator. At the end of the incubation time, 3.0 x 10^4 Vero cells in 100 µL of MEM with 2% FBS were added to each well, and the plates were incubated at 37°C in a humidified CO_2 incubator. After 3 days of incubation, the plates were emptied and hand-washed twice with DPBS. Fixation was performed by adding 100 µL of a cold 80% vol/vol solution of Acetone (Sigma-Merck) in DPBS and incubating the plates for 10 min at RT. After the incubation period, the plates were emptied and air dried. The ELISA test was performed on the same day as fixation. Plates were washed 3 times by means of an automatic plate washer (each well was washed with 300 µL/well of wash buffer prepared with DPBS + 0.3% of Tween 20 (Sigma-Merck)) and 100 µL/well of the primary antibody solution was added. The primary antibody,

Anti-RSV Antibody, clones 133-1H, 131-2G, and 130-12H (Sigma-Merck) was diluted in a 1:10 000 ratio by using the antibody diluent (a 5% non-fat dried milk solution in wash buffer). Plates were incubated for 1 hour at RT. Subsequently, the plates were washed three times, as previously, and 100 µL of the secondary antibody solution - Goat Anti-Mouse IgG (H+L)-HRP Conjugate (Bio-Rad) diluted in a 1:2 000 ratio in the antibody diluent - was then added and the plates were incubated for 1 hour in the dark at RT. Next, the plates were automatically washed for the third time (6 rinses with 300 µl of wash buffer per well) and 100 µL of the substrate solution was added to each well. The substrate solution had previously been prepared by adding one o-Phenylenediamine dihydrochloride tablet (OPD, Sigma-Merck) to 20 mL of a citrate buffer. The plates were incubated for 10 minutes at RT in the dark. The reaction was stopped by adding 100 µL of stop solution (2.8% vol/vol Sulfuric Acid (Sigma-Merck) in distilled water) and the plates were read at an optical density of 490 nm (OD490) by means of a SpectraMax ELISA plate (Medical Device) reader.

9.3. Validation parameters

Each sample was tested in four different analytical sessions run by two operators over two days with three replicate measurements per session. For each of the three replicate measurements, a geometric mean titer (GMT) was calculated. The validation testing design is shown in Figure 22.

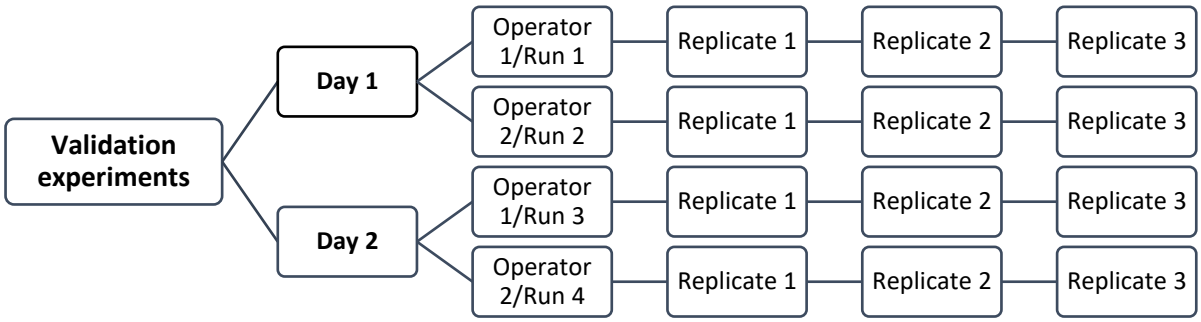

Figure 22: Validation testing design.

Linearity

Linearity was assessed by testing the sample in a 2-fold dilution scheme in which at least one dilution had a titer below the lower limit of quantitation of the assay, starting from a dilution of 1:20. Thus, as the sample in the first well was diluted 1:20, the starting dilution in the first well was 1:20, 1:40, 1:80, 1:160, 1:320, 1:640, 1:1280, 1:2560, 1:5120, 1:10240, 1:20480 and

1:40960. The above-mentioned sample dilutions were tested in one repetition per plate, in three different plates by two different operators on day 1 and day 2.

The parameter was evaluated by examining the relationship between the base-2 logarithm of the GMT (observed titers) and the base-2 logarithm of the serum dilutions across the factorial design. The coefficient of determination (R^2), y-intercept and slope of the regression line were calculated and reported.

Relative accuracy

The accuracy of the test was evaluated by using the reportable (RP) values obtained during the evaluation of Linearity. The accuracy can be tested by using either a conventional true value or an accepted reference value [60]. The GMT of the expected values was calculated from the GMT of the results obtained from the neat sample, and by dividing this value by the corresponding factor of the 2-fold serial dilution.

Relative accuracy was evaluated by calculating the percentage of recovery on the GMT of the RP values and the expected (true) titer and applying the formula: *100*(GMT observed / GMT expected)*.

Precision

Precision was assessed by using the results yielded by the linearity tests. Three aspects of precision were considered: repeatability, intermediate precision and format variability.

Precision – Repeatability

Intra-run variability, or repeatability, is the variation expected across replicates under the same operating conditions over a short period of time (28).

Precision – Intermediate Precision

Intermediate precision is determined from the total variance component. It indicates the variations and random events that can occur within laboratories, such as days, environmental conditions, operators and equipment.

Precision – Format Variability

Format variability represents the variation expected across GMT results yielded by multiple replicates in routine testing. For its calculation, we considered two independent runs consisting of one replicate.

Limit of Quantitation and Range

The lower (LLOQ) and upper (ULOQ) Limits of Quantitation were determined as the lower and upper 95% CI of the observed GMT of the lowest and highest sample concentrations at which the assay yielded linear, accurate and precise results.

Specificity

Specificity was assessed by testing anti-homologous and anti-heterologous serum samples. The positive sample for the homologous strain had to show a 4-fold difference from the heterologous strains tested.

Robustness

The robustness of an analytical procedure is its capacity to remain unaffected by small but deliberate variations during measurements and gives an indication of its reliability.
Two critical conditions were evaluated: cell suspension concentrations and virus-serum mixture incubation time.

9.4. Results

9.4.1. RSV propagation set-up

The virus propagation setup for both RSV subtypes used two different cell lines, HEp-2 and Vero cells [100]. Initially, both lines were widely used to study RSV infection, proving permissive to RSV and sensitive to different RSV subtypes, as shown in Figure 23.
However, as documented in various studies, the Vero cell-grown virus can infect human airway epithelial cell cultures 600-fold less efficiently than the HEp-2 cell-grown virus [101].
In addition, a fluctuating loss of infectivity by both RSV subtypes was observed, which can be explained by particle instability and aggregation caused by freeze-thawing and handling. It has been demonstrated that many sugars, of which sucrose seems to have a more impactful effect, are able to preserve the viability of viruses during freeze-thaw cycles and to avoid RSV

aggregation [102]. The best MN titers with the highest stability were obtained with HEp-2 cell-grown virus and the optimal sucrose concentration was 3%.

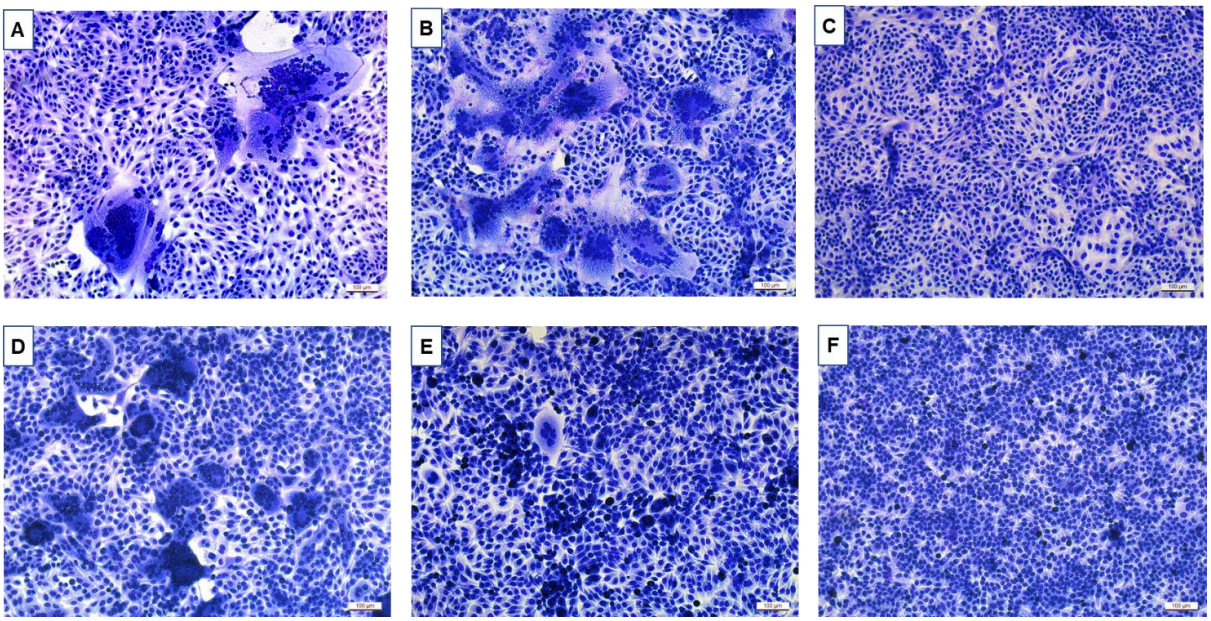

Figure 23: Different pictures of syncytia caused by RSV A infection in Vero cell line (A) and HEp-2 cell line (D), by RSV B infection in Vero cell line (B) and HEp-2 cell line (E) and control cells in Vero cell line (C) and HEp-2 cell line (F).

9.4.2. Set-up and validation of MN assay

Before the validation experiments, a series of preliminary analyses was performed to select the optimal conditions. To this end, different types of cell lines were used - Vero and HEp-2 - at different concentrations (150K and 300K cell/mL); both cell suspension and cell adhesion were then tested. The use of different cell media was also investigated by using both the MEM w/ Earle's Salts w/o L-Glutamine medium (MEM) and DMEM. The most suitable MN incubation time was then investigated on days 2, 3, 4 and 5. Finally, a cross test was performed in order to find the best primary and secondary antibody concentrations. The optimal combination was: Vero cells at a concentration of 300K cell/mL, cell suspension with MEM medium and 3-day incubation. The best concentration of the primary antibody was 1:10 000, while that of the secondary HRP conjugated anti-mouse IgG was 1:2 000.

9.4.3. Linearity

Linearity is assessed in order to demonstrate that a high concentration of the sample of interest can be diluted to a concentration within the working range and still give a reliable result [62].

The MN assay is considered to have acceptable linearity if, for each RSV subtype, the 95% confidence interval of the slope is between 0.7 and 1.3. In the present study, R^2 was close to 1 for both RSV-A and B, whereas the absolute values of the slope were 1.014 and 1.001, respectively. Results are reported in Figure 24.

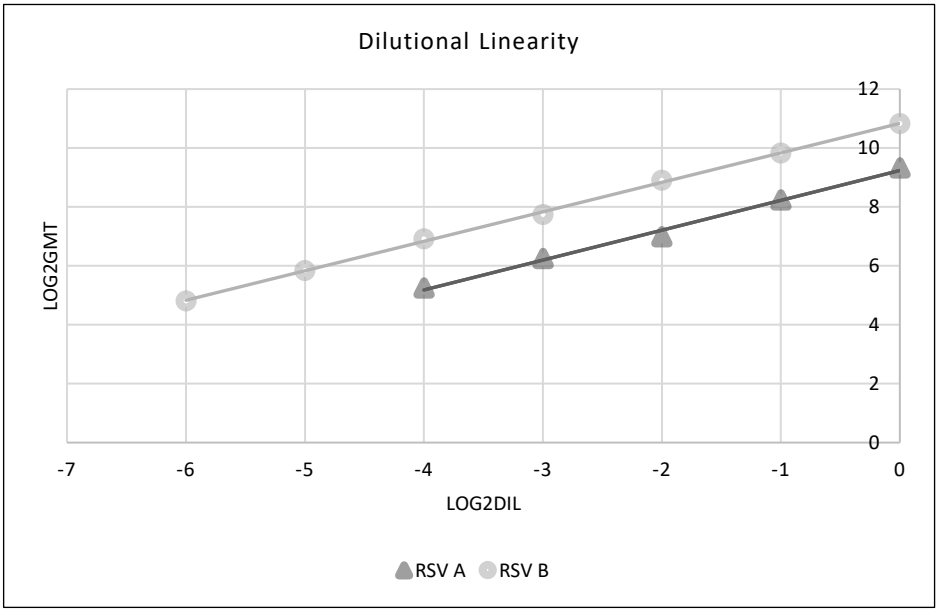

Figure 24: Dilutional linearity graph for RSV-A and B, showing the logarithm of the dilutions on the X axis and the logarithm of the obtained GMT on the Y-axis.

9.4.4. Relative accuracy

The assay is considered to have acceptable relative accuracy if the observed GMT of all replicates obtained for a sample is within ±50% to 200% of the expected titer. The MN assay is accurate from 1:1 to 1:16 dilution for RSV-A and from 1:1 to 1:64 dilution for RSV-B, as shown in Table 15.

Table 15: Relative accuracy results for RSV-A (1) and RSV-B (2).

1			
Fold dilution	**Observed GMT**	**Expected GMT**	**Relative accuracy**
1	640	640	100%
2	302	320	94%
4	127	160	79%
8	76	80	95%
16	38	40	95%

2			
Fold dilution	**Observed GMT**	**Expected GMT**	**Relative accuracy**
1	1810	1810	100%
2	905	905	100%
4	479	453	106%
8	214	226	95%
16	120	113	106%
32	57	57	100%
64	28	28	100%

9.4.5. Precision

9.4.5.1. Repeatability

The assay is considered to have acceptable repeatability if all samples display a percentage geometric coefficient of variation (%GCV) ≤65.5%. The results shown in Table 16 indicate that the MN assay is repeatable from 1:1 to 1:16 dilution for RSV-A and from 1:1 to 1:64 dilution for RSV-B.

Table 16: Repeatability (intra-run) results for RSV-A (1) and RSV-B (2).

1		
Fold dilution	**Observed GMT**	**Repeatability**
1	640	0%
2	302	22%
4	127	40%
8	76	22%
16	38	22%

2		
Fold dilution	**Observed GMT**	**Repeatability**
1	1810	41%
2	905	33%
4	479	22%
8	214	33%
16	120	38%
32	57	33%
64	28	44%

9.4.5.2. Intermediate precision

The assay is deemed to be precise if all estimates of intermediate precision display %GCV ≤ 129.0%. The results reported in Table 17 indicate that the MN assay is precise from 1:1 to 1:16 dilution for RSV-A and from 1:1 to 1:64 dilution for RSV-B.

Table 17: Intermediate precision results for RSV-A (1) and RSV-B (2).

1		
Fold dilution	**Observed GMT**	**Intermediate precision**
1	640	0.0%
2	302	22.2%
4	127	41.4%
8	76	22.2%
16	38	22.2%

2		
Fold dilution	**Observed GMT**	**Intermediate precision**
1	1810	44.1%
2	905	51.7%
4	479	56.4%
8	214	46.7%
16	120	46.7%
32	57	51.7%
64	28	43.6%

9.4.5.3. Format variability

The MN assay is considered to have acceptable format variability if all samples display %GCV ≤81.5%; the criterion was met for both RSV subtypes, as reported in Table 18.

Table 18: Format variability results for RSV-A (1) and RSV-B (2).

1		
Fold dilution	**Observed GMT**	**Format variability**
1	640	0.0%
2	302	15.2%
4	127	27.8%
8	76	15.2%
16	38	15.2%

2		
Fold dilution	**Observed GMT**	**Format variability**
1	1810	29.5%
2	905	34.2%
4	479	37.2%
8	214	31.1%
16	120	31.1%
32	57	34.2%
64	28	29.2%

9.4.6. Limit of quantitation and range

For RSV-A, the LLOQ is set at 20 and the ULOQ is set at 640. For RSV-B, the LLOQ is set at 20, while the ULOQ is set at 2560.

9.4.7. Specificity

To determine the specificity, positive samples for homologous (HS) and heterologous (HET) viruses were tested as reported in Table 16. The positive homologous sample showed a GMT with at least a four-fold difference from the heterologous samples. The negative sample showed negative titers in all measurements of this parameter.

The results reported in Table 19 indicate that the MN assay is specific.

Table 19: Specificity results for RSV-A and RSV-B showing the fold-change.

	HS/HET 1 (GMT)	**HS/HET 2 (GMT)**	**HS/HET 3 (GMT)**
RSV A	32	32	32
RSV B	16	16	16

9.4.8. Robustness

Two different cell suspension concentrations were used for each subtype: the standard concentration (3.0 x 10^4 cell/mL) and a non-standard concentration (1.5 x 10^4 cell/mL). Samples were tested in four replicates/plate, each by two different operators for each

condition, thus obtaining sixteen titer values. The results obtained in each condition were aggregated to obtain eight RP values for each sample.

Plates were incubated for 60 min with the virus solution (standard condition) before the addition of the cell suspension; to assess the influence of the incubation time, plates were incubated with the viral solution for 45- and 75-min. Samples were tested in four replicates/plate by two different operators for each condition, thus obtaining twenty-four titer values. Results obtained from each condition were combined to obtain twelve RP values for each sample.

Regarding the cell suspension concentration, the %GCV was 19.65% for RSV-A and 17.40% for RSV-B, thus meeting the acceptance criterion set at ≤45%. With regard to the effect of the incubation time, the %GCV was 18.61% for RSV-A and 16.97% for RSV-B, thus meeting the acceptance criterion set at ≤45%. The above-mentioned results, together with the negative control, which showed negative titers, indicate that the MN assay is robust (Table 20).

Table 20: Robustness results for RSV-A and RSV-B, with standard deviation (SD) and % geometric coefficient of variation (GCV).

	Cell suspension concentration		**Virus-serum mixture incubation time**	
	SD	**%GCV**	**SD**	**%GCV**
RSV A	0.2	19.65	0.2	18.61
RSV B	0.2	17.40	0.2	16.97

9.5. Discussion

This study aims to provide guidelines and criteria for the establishment of a standard operating procedure for a high-throughput RSV neutralization assay. In the serological field, it is important to have specific serological assays that can assess the efficacy of vaccines and antiviral drugs, evaluate monoclonal antibodies (mAbs) and establish new correlates of protections (CoP). The first step towards achieving these goals is to establish a common assay protocol. The definition of well-established CoP, especially mechanistic CoP, is a fundamental step towards designing better and more effective vaccines. Moreover, it is essential to understanding basic immunology and determining the susceptibility of a single individual or a population.

RSV has a high impact in infants, immunocompromised subjects and the elderly worldwide, in terms of death, hospitalization and the need for intensive care. Nevertheless, only two

candidate vaccines have been approved for use in adults ages 60 and over so far by FDA. This is probably due to the former reluctance of manufacturers to invest in new candidate vaccines, because of the high costs and the risk of serious adverse effects, such as the dramatic effects elicited by the first formalin-inactivated RSV vaccine in the 1960s.

The RSV MN assay is the most widely used method, since neutralizing antibodies play a key role in protecting against RSV infection and constitute the best correlates of protection. Thus, investigating the activity of nAb in depth could be of great value to the development of vaccines and new drugs against RSV, as happened in the case of SARS-CoV-2 vaccines immediately after the outbreak [46].

In addition to MN assay, binding assays, such as ELISA or Multiplexing assays in general, could be a valid surrogate for the neutralizing assays, as they are able to increase sample throughput. The main drawback is that they require the correct protein conformation of the F antigen (Pre-F). At present, the technologies for stabilizing and producing this type of antigen seem to be restricted, owing to patent pending issues. Moreover, the establishment of a possible CoP for RSV should be based on the neutralizing response, since a high correlation between virus-specific functional neutralizing antibody titers and protection against the disease has been demonstrated. Thus, the aim was to describe the development of a validated assay and to underline the importance of a bioanalytical serological method able to specifically quantitate the presence of nAb after natural infection and/or vaccination [40].

10. CONCLUSIONS

Among many strategies available today to counter viral infections, vaccines are the best tool for prevention especially for groups of subjects having high risk of secondary complications like infants, elderly, immune-compromised patients, and pregnant women. Cell mediated and humoral responses, together with molecular and serological assays are some of the main bioanalytical methods that can produce data supporting the submission to a specific regulatory agency by the pharmaceutical company manufacturing the vaccine candidate.

In the present study three different approaches of validation design have been analysed and reported. Each validation scheme has specific parameter and acceptance criteria to be met depending on the technical features of the applied method (flow cytometry, Real Time RT-PCR and Microneutralization assays).

Generally, more than one method is required to produce reliable data supporting the license of a new candidate vaccine. In this case, flow cytometry gave an estimation of the humoral response and the immunogenicity, molecular biology (analysis of the presence/absence of the target of interest) contributed to assess the efficacy of vaccination and the microneutralization assay detected the presence of nAb contributing to the immunogenicity evaluation.

Given the impact of the above-mentioned methods, the standardization and validation processes, performed according to well-defined international guidelines, are a key step to providing reliable results, especially when the assay is used to analyse samples from official clinical trials. In addition, it would be beneficial to use official WHO international standards, when available, in order to be able to properly standardize the assay and compare results from different laboratories and different assay formats. This aspect would be a great advantage in the future to assess the efficacy and immunogenicity of new candidate vaccines as well as in sero-epidemiological studies for the definition of CoP.

11. APPENDIX

Table 1: Relative accuracy percentages for each dilution for each strain in each duplex analysis.

H1pdm09 *vs* B/Victoria			
A/Sing			
Fold dilution	*Observed GMCt*	*Expected GMCt*	*Relative Accuracy*
10^0	12.3	12.3	100%
10^1	15.4	15.6	99%
10^2	18.7	18.9	99%
10^3	22.0	22.2	99%
10^4	25.8	25.5	101%
10^5	28.9	28.8	100%
10^6	32.2	32.1	100%
10^7	35.1	35.4	99%
A/Bris			
Fold dilution	*Observed GMCt*	*Expected GMCt*	*Relative Accuracy*
10^0	14.4	14.4	100%
10^1	17.6	17.7	99%
10^2	20.9	21.0	100%
10^3	24.2	24.3	100%
10^4	27.9	27.6	101%
10^5	31.2	30.9	101%
10^6	34.4	34.2	101%
10^7	37.1	37.5	99%
A/Idaho			
Fold dilution	*Observed GMCt*	*Expected GMCt*	*Relative Accuracy*
10^0	14.1	14.1	100%
10^1	17.2	17.4	99%
10^2	20.5	20.7	99%
10^3	24.0	24.0	100%
10^4	27.4	27.3	100%
10^5	30.7	30.6	100%
10^6	34.1	33.9	101%
10^7	37.6	37.2	101%
B/Iowa			

Fold dilution	*Observed GMCt*	*Expected GMCt*	*Relative Accuracy*
10^0	11.3	11.3	100%
10^1	14.4	14.6	99%
10^2	17.7	17.9	99%
10^3	20.9	21.2	99%
10^4	24.4	24.5	100%
10^5	27.9	27.8	100%
10^6	31.0	31.1	100%
10^7	34.2	34.4	99%
B/Colo			
Fold dilution	*Observed GMCt*	*Expected GMCt*	*Relative Accuracy*
10^0	13.5	13.5	100%
10^1	16.6	16.8	99%
10^2	19.9	20.1	99%
10^3	23.2	23.4	99%
10^4	26.7	26.7	100%
10^5	29.9	30.0	100%
10^6	33.2	33.3	100%
10^7	36.7	36.6	100%
B/Bris			
Fold dilution	*Observed GMCt*	*Expected GMCt*	*Relative Accuracy*
10^0	12.6	12.6	100%
10^1	15.7	15.9	99%
10^2	18.9	19.2	98%
10^3	22.7	22.5	101%
10^4	25.3	25.8	98%
10^5	28.9	29.1	99%
10^6	32.2	32.4	99%
10^7	35.4	35.7	99%
H3N2 *vs* B/Yamagata			
A/North			
Fold dilution	*Observed GMCt*	*Expected GMCt*	*Relative Accuracy*
10^0	13.5	13.5	100%
10^1	16.6	16.8	99%
10^2	19.9	20.1	99%

10^3	23.1	23.4	99%
10^4	26.4	26.7	99%
10^5	29.8	30.0	99%
10^6	33.5	33.3	101%
10^7	36.7	36.6	100%
A/Ind			
Fold dilution	*Observed GMCt*	*Expected GMCt*	*Relative Accuracy*
10^0	12.0	12.0	100%
10^1	15.1	15.3	99%
10^2	18.4	18.6	99%
10^3	21.7	21.9	99%
10^4	25.0	25.2	99%
10^5	28.3	28.5	99%
10^6	32.0	31.8	101%
10^7	35.6	35.1	101%
A/HK			
Fold dilution	*Observed GMCt*	*Expected GMCt*	*Relative Accuracy*
10^0	13.4	13.4	100%
10^1	16.4	16.7	98%
10^2	19.7	20.0	99%
10^3	23.0	23.3	99%
10^4	26.3	26.6	99%
10^5	29.7	29.9	99%
10^6	33.6	33.2	101%
10^7	37.1	36.5	102%
B/Sing			
Fold dilution	*Observed GMCt*	*Expected GMCt*	*Relative Accuracy*
10^0	13.1	13.1	100%
10^1	16.2	16.4	99%
10^2	19.6	19.7	99%
10^3	22.8	23.0	99%
10^4	26.0	26.3	99%
10^5	29.3	29.6	99%
10^6	32.9	32.9	100%
10^7	36.1	36.2	100%

B/Utah			
Fold dilution	*Observed GMCt*	*Expected GMCt*	*Relative Accuracy*
10^0	19.4	19.4	100%
10^1	21.7	22.7	96%
10^2	25.0	26.0	96%
10^3	28.3	29.3	97%
10^4	31.5	32.6	97%
10^5	34.7	35.9	97%
10^6	38.5	39.2	Not applicable
10^7	39.8	42.5	Not applicable
B/Mass			
Fold dilution	*Observed GMCt*	*Expected GMCt*	*Relative Accuracy*
10^0	12.6	12.6	100%
10^1	15.7	15.9	99%
10^2	18.9	19.2	98%
10^3	22.2	22.5	99%
10^4	25.5	25.8	99%
10^5	28.8	29.1	99%
10^6	32.3	32.4	100%
10^7	36.2	35.7	101%
H1pdm09 *vs* H3N2			
A/Sing			
Fold dilution	*Observed GMCt*	*Expected GMCt*	*Relative Accuracy*
10^0	11.2	11.2	100%
10^1	14.4	14.5	99%
10^2	17.6	17.8	99%
10^3	20.9	21.1	99%
10^4	24.4	24.4	100%
10^5	27.6	27.7	100%
10^6	32.7	31.0	Not applicable
10^7	40.0	34.3	Not applicable
A/Bris			
Fold dilution	*Observed GMCt*	*Expected GMCt*	*Relative Accuracy*
10^0	12.7	12.7	100%

10^1	15.8	16.0	99%
10^2	19.0	19.3	98%
10^3	22.3	22.6	99%
10^4	25.8	25.9	100%
10^5	30.5	29.2	104%
10^6	38.8	32.5	Not applicable
10^7	40.0	35.8	Not applicable
A/Idaho			
Fold dilution	*Observed GMCt*	*Expected GMCt*	*Relative Accuracy*
10^0	12.6	12.6	100%
10^1	15.8	15.9	99%
10^2	19.1	19.2	99%
10^3	22.3	22.5	99%
10^4	25.8	25.8	100%
10^5	30.4	29.1	104%
10^6	37.2	32.4	Not applicable
10^7	40.0	35.7	Not applicable
A/North			
Fold dilution	*Observed GMCt*	*Expected GMCt*	*Relative Accuracy*
10^0	12.3	12.3	100%
10^1	15.5	15.6	99%
10^2	18.8	18.9	99%
10^3	22.2	22.2	100%
10^4	25.8	25.5	101%
10^5	29.1	28.8	101%
10^6	34.1	32.1	Not applicable
10^7	40.0	35.4	Not applicable
A/Ind			
Fold dilution	*Observed GMCt*	*Expected GMCt*	*Relative Accuracy*
10^0	11.6	11.6	100%
10^1	14.9	14.9	100%
10^2	18.1	18.2	99%
10^3	21.4	21.5	100%
10^4	25.1	24.8	101%
10^5	27.8	28.1	99%

10^6	32.2	31.4	103%
10^7	38.3	34.7	Not applicable
A/HK			
Fold dilution	*Observed GMCt*	*Expected GMCt*	*Relative Accuracy*
10^0	12.9	12.9	100%
10^1	16.0	16.2	99%
10^2	19.4	19.5	99%
10^3	22.6	22.8	99%
10^4	26.3	26.1	101%
10^5	30.8	29.4	105%
10^6	36.0	32.7	Not applicable
10^7	40.0	36.0	Not applicable
B/Victoria *vs* B/Yamagata			
B/Iowa			
Fold dilution	*Observed GMCt*	*Expected GMCt*	*Relative Accuracy*
10^0	11.7	11.7	100%
10^1	14.9	15.0	99%
10^2	18.2	18.3	99%
10^3	21.6	21.6	100%
10^4	24.7	24.9	99%
10^5	27.9	28.2	99%
10^6	31.0	31.5	98%
10^7	33.7	34.8	97%
B/Colo			
Fold dilution	*Observed GMCt*	*Expected GMCt*	*Relative Accuracy*
10^0	13.5	13.5	100%
10^1	16.9	16.8	101%
10^2	20.2	20.1	100%
10^3	23.5	23.4	100%
10^4	26.7	26.7	100%
10^5	29.9	30.0	100%
10^6	33.0	33.3	99%
10^7	37.4	36.6	102%
B/Colo			

Fold dilution	*Observed GMCt*	*Expected GMCt*	*Relative Accuracy*
10^0	12.6	12.6	100%
10^1	15.8	15.9	99%
10^2	19.1	19.2	99%
10^3	22.3	22.5	99%
10^4	25.6	25.8	99%
10^5	28.9	29.1	99%
10^6	32.2	32.4	99%
10^7	35.3	35.7	99%
B/Sing			
Fold dilution	*Observed GMCt*	*Expected GMCt*	*Relative Accuracy*
10^0	12.9	12.9	100%
10^1	16.1	16.2	99%
10^2	19.5	19.5	100%
10^3	22.8	22.8	100%
10^4	26.1	26.1	100%
10^5	29.3	29.4	100%
10^6	32.5	32.7	99%
10^7	36.3	36.0	101%
B/Utah			
Fold dilution	*Observed GMCt*	*Expected GMCt*	*Relative Accuracy*
10^0	12.4	12.4	100%
10^1	15.6	15.7	99%
10^2	18.9	19.0	99%
10^3	22.2	22.3	100%
10^4	25.5	25.6	100%
10^5	28.8	28.9	100%
10^6	32.1	32.2	100%
10^7	35.2	35.5	99%
B/Mass			
Fold dilution	*Observed GMCt*	*Expected GMCt*	*Relative Accuracy*
10^0	13.9	13.9	100%
10^1	17.1	17.2	99%
10^2	20.3	20.5	99%
10^3	23.6	23.8	99%

10^4	26.7	27.1	99%
10^5	30.5	30.4	100%
10^6	32.9	33.7	98%
10^7	36.2	37.0	98%

Table 2: Precision (repeatability, intermediate precision, and format variability) for each dilution for each strain in each duplex analysis

H1pdm09 *vs* B/Victoria				
A/Sing				
Fold dilution	*Observed GMCt*	*Repeatability*	*Intermediate precision*	*Format variability*
10^0	12.3	0.5%	2.1%	2.1%
10^1	15.4	0.3%	1.8%	1.8%
10^2	18.7	0.2%	1.7%	1.7%
10^3	22.0	0.3%	1.3%	1.3%
10^4	25.8	0.3%	2.6%	2.5%
10^5	28.9	0.3%	2.1%	2.1%
10^6	32.2	0.6%	1.8%	1.7%
10^7	35.1	3.9%	3.9%	2.2%
A/Bris				
Fold dilution	*Observed GMCt*	*Repeatability*	*Intermediate precision*	*Format variability*
10^0	14.4	0.3%	2.9%	2.9%
10^1	17.6	0.1%	2.4%	2.4%
10^2	20.9	0.2%	1.9%	1.9%
10^3	24.2	0.2%	1.6%	1.5%
10^4	27.9	0.3%	2.2%	2.2%
10^5	31.2	0.2%	2.1%	2.1%
10^6	34.4	1.2%	1.8%	1.5%
10^7	37.1	8.7%	9.1%	5.6%
A/Idaho				
Fold dilution	*Observed GMCt*	*Repeatability*	*Intermediate precision*	*Format variability*
10^0	14.1	0.4%	2.5%	2.5%

10^1	17.2	0.3%	2.1%	2.0%
10^2	20.5	0.3%	1.8%	1.8%
10^3	24.0	0.2%	3.4%	3.4%
10^4	27.4	0.6%	2.9%	2.8%
10^5	30.7	0.2%	2.9%	2.9%
10^6	34.1	0.8%	3.4%	3.3%
10^7	37.6	3.1%	3.4%	2.3%
B/Iowa				
Fold dilution	*Observed GMCt*	*Repeatability*	*Intermediate precision*	*Format variability*
10^0	11.3	0.6%	4.3%	4.3%
10^1	14.4	0.4%	3.4%	3.4%
10^2	17.7	0.5%	2.7%	2.6%
10^3	20.9	0.3%	2.3%	2.3%
10^4	24.4	0.2%	2.0%	2.0%
10^5	27.9	0.4%	2.7%	2.7%
10^6	31.0	0.4%	2.2%	2.2%
10^7	34.2	1.2%	2.1%	1.8%
B/Colo				
Fold dilution	*Observed GMCt*	*Repeatability*	*Intermediate precision*	*Format variability*
10^0	13.5	0.8%	2.8%	2.7%
10^1	16.6	0.3%	2.0%	2.0%
10^2	19.9	0.2%	1.9%	1.9%
10^3	23.2	0.3%	1.8%	1.7%
10^4	26.7	0.2%	2.6%	2.6%
10^5	29.9	0.2%	2.1%	2.1%
10^6	33.2	0.8%	2.3%	2.2%
10^7	36.7	2.8%	3.9%	3.2%
B/Bris				
Fold dilution	*Observed GMCt*	*Repeatability*	*Intermediate precision*	*Format variability*
10^0	12.6	0.6%	3.3%	3.3%
10^1	15.7	0.8%	2.6%	2.5%
10^2	18.9	0.2%	2.2%	2.2%

10^3	22.7	3.9%	8.6%	7.9%
10^4	25.3	0.4%	1.7%	1.7%
10^5	28.9	0.3%	2.0%	2.0%
10^6	32.2	0.8%	2.2%	2.1%
10^7	35.4	1.7%	2.4%	1.9%
H3N2 *vs* B/Yamagata				
A/North				
Fold dilution	*Observed GMCt*	*Repeatability*	*Intermediate precision*	*Format variability*
10^0	13.5	0.5%	1.4%	1.4%
10^1	16.6	0.3%	1.1%	1.0%
10^2	19.9	0.3%	0.9%	0.8%
10^3	23.1	0.2%	0.6%	0.6%
10^4	26.4	0.2%	0.6%	0.6%
10^5	29.8	0.2%	0.9%	0.9%
10^6	33.5	0.5%	1.6%	1.5%
10^7	36.7	2.0%	2.3%	1.6%
A/Ind				
Fold dilution	*Observed GMCt*	*Repeatability*	*Intermediate precision*	*Format variability*
10^0	12.0	0.6%	2.2%	2.1%
10^1	15.1	0.3%	1.6%	1.5%
10^2	18.4	0.3%	1.4%	1.3%
10^3	21.7	0.3%	1.3%	1.3%
10^4	25.0	0.3%	1.1%	1.1%
10^5	28.3	0.8%	1.5%	1.3%
10^6	32.0	0.4%	2.4%	2.4%
10^7	35.6	1.2%	2.1%	1.9%
A/HK				
Fold dilution	*Observed GMCt*	*Repeatability*	*Intermediate precision*	*Format variability*
10^0	13.4	0.3%	2.7%	2.7%
10^1	16.4	0.4%	2.2%	2.2%
10^2	19.7	0.2%	1.8%	1.8%

10^3	23.0	0.2%	1.7%	1.7%
10^4	26.3	0.1%	1.5%	1.5%
10^5	29.7	0.2%	1.6%	1.6%
10^6	33.6	0.5%	2.0%	2.0%
10^7	37.1	1.6%	2.1%	1.6%
B/Sing				
Fold dilution	*Observed GMCt*	*Repeatability*	*Intermediate precision*	*Format variability*
10^0	13.1	0.8%	2.9%	2.9%
10^1	16.2	0.3%	2.3%	2.3%
10^2	19.6	0.4%	1.7%	1.7%
10^3	22.8	0.4%	1.5%	1.4%
10^4	26.0	0.2%	1.4%	1.3%
10^5	29.3	0.3%	1.2%	1.2%
10^6	32.9	0.7%	1.6%	1.5%
10^7	36.1	1.5%	2.4%	2.1%
B/Utah				
Fold dilution	*Observed GMCt*	*Repeatability*	*Intermediate precision*	*Format variability*
10^0	19.4	0.7%	2.6%	2.5%
10^1	21.7	0.4%	2.2%	2.2%
10^2	25.0	0.3%	1.8%	1.8%
10^3	28.3	0.4%	1.6%	1.6%
10^4	31.5	0.7%	1.5%	1.4%
10^5	34.7	1.5%	2.0%	1.5%
10^6	38.5	Not applicable	Not applicable	Not applicable
10^7	39.8	Not applicable	Not applicable	Not applicable
B/Mass				
Fold dilution	*Observed GMCt*	*Repeatability*	*Intermediate precision*	*Format variability*
10^0	12.6	0.4%	3.1%	3.1%
10^1	15.7	0.3%	2.5%	2.5%
10^2	18.9	0.3%	2.0%	2.0%
10^3	22.2	0.3%	1.8%	1.8%
10^4	25.5	0.1%	1.6%	1.6%

10^5	28.8	0.3%	1.4%	1.4%
10^6	32.3	0.6%	2.0%	1.9%
10^7	36.2	2.0%	2.4%	1.7%
H1pdm09 *vs* H3N2				
A/Sing				
Fold dilution	*Observed GMCt*	*Repeatability*	*Intermediate precision*	*Format variability*
10^0	11.2	0.4%	5.0%	5.0%
10^1	14.4	0.2%	3.7%	3.7%
10^2	17.6	0.2%	2.9%	2.9%
10^3	20.9	0.2%	2.4%	2.4%
10^4	24.4	0.1%	2.3%	2.3%
10^5	27.6	0.2%	2.7%	2.7%
10^6	32.7	Not applicable	Not applicable	Not applicable
10^7	40.0	Not applicable	Not applicable	Not applicable
A/Bris				
Fold dilution	*Observed GMCt*	*Repeatability*	*Intermediate precision*	*Format variability*
10^0	12.7	0.3%	5.9%	5.9%
10^1	15.8	0.4%	4.7%	4.7%
10^2	19.0	0.2%	4.1%	4.1%
10^3	22.3	0.1%	3.5%	3.5%
10^4	25.8	0.1%	3.2%	3.2%
10^5	30.5	0.3%	12.5%	12.5%
10^6	38.8	Not applicable	Not applicable	Not applicable
10^7	40.0	Not applicable	Not applicable	Not applicable
A/Idaho				
Fold dilution	*Observed GMCt*	*Repeatability*	*Intermediate precision*	*Format variability*
10^0	12.6	0.4%	5.8%	5.8%
10^1	15.8	0.2%	4.7%	4.7%
10^2	19.1	0.1%	3.9%	3.9%
10^3	22.3	0.1%	3.4%	3.4%
10^4	25.8	0.1%	3.4%	3.4%

10^5	30.4	0.4%	12.7%	12.7%
10^6	37.2	Not applicable	Not applicable	Not applicable
10^7	40.0	Not applicable	Not applicable	Not applicable
A/North				
Fold dilution	*Observed GMCt*	*Repeatability*	*Intermediate precision*	*Format variability*
10^0	12.3	0.6%	2.7%	2.7%
10^1	15.5	0.4%	2.5%	2.5%
10^2	18.8	0.3%	1.9%	1.9%
10^3	22.2	0.2%	2.2%	2.2%
10^4	25.8	0.2%	3.6%	3.6%
10^5	29.1	0.3%	4.0%	3.9%
10^6	34.1	Not applicable	Not applicable	Not applicable
10^7	40.0	Not applicable	Not applicable	Not applicable
A/Ind				
Fold dilution	*Observed GMCt*	*Repeatability*	*Intermediate precision*	*Format variability*
10^0	11.6	1.1%	4.5%	4.4%
10^1	14.9	0.3%	3.4%	3.4%
10^2	18.1	0.4%	2.9%	2.8%
10^3	21.4	0.2%	2.6%	2.6%
10^4	25.1	0.2%	3.5%	3.5%
10^5	27.8	0.3%	3.0%	3.0%
10^6	32.2	4.8%	11.4%	10.6%
10^7	38.3	Not applicable	Not applicable	Not applicable
A/HK				
Fold dilution	*Observed GMCt*	*Repeatability*	*Intermediate precision*	*Format variability*
10^0	12.9	0.4%	3.4%	3.4%
10^1	16.0	0.3%	2.9%	2.9%
10^2	19.4	0.2%	2.3%	2.2%
10^3	22.6	0.1%	2.1%	2.1%
10^4	26.3	0.5%	2.8%	2.8%
10^5	30.8	0.4%	12.3%	12.2%
10^6	36.0	Not applicable	Not applicable	Not applicable

10^7	40.0	Not applicable	Not applicable	Not applicable
B/Victoria *vs* B/Yamagata				
B/Iowa				
Fold dilution	*Observed GMCt*	*Repeatability*	*Intermediate precision*	*Format variability*
10^0	11.7	1.3%	2.1%	1.8%
10^1	14.9	0.5%	1.6%	1.6%
10^2	18.2	0.3%	1.3%	1.2%
10^3	21.6	0.2%	2.1%	2.1%
10^4	24.7	0.2%	0.9%	0.8%
10^5	27.9	0.3%	0.8%	0.8%
10^6	31.0	0.3%	0.9%	0.8%
10^7	33.7	0.7%	1.1%	1.0%
B/Colo				
Fold dilution	*Observed GMCt*	*Repeatability*	*Intermediate precision*	*Format variability*
10^0	13.5	1.3%	2.7%	2.4%
10^1	16.9	0.3%	1.8%	1.7%
10^2	20.2	0.4%	1.6%	1.5%
10^3	23.5	0.2%	1.3%	1.3%
10^4	26.7	0.2%	1.0%	1.0%
10^5	29.9	0.2%	0.9%	0.9%
10^6	33.0	0.9%	1.0%	0.7%
10^7	37.4	5.7%	6.3%	4.1%
B/Bris				
Fold dilution	*Observed GMCt*	*Repeatability*	*Intermediate precision*	*Format variability*
10^0	12.6	0.7%	4.3%	4.3%
10^1	15.8	0.5%	3.1%	3.1%
10^2	19.1	0.3%	2.5%	2.5%
10^3	22.3	0.3%	2.1%	2.1%
10^4	25.6	0.4%	1.9%	1.9%
10^5	28.9	0.3%	1.5%	1.5%
10^6	32.2	0.6%	1.5%	1.4%

10^7	35.3	2.9%	3.5%	2.6%
B/Sing				
Fold dilution	*Observed GMCt*	*Repeatability*	*Intermediate precision*	*Format variability*
10^0	12.9	0.8%	3.0%	2.9%
10^1	16.1	0.4%	2.4%	2.3%
10^2	19.5	0.5%	2.2%	2.1%
10^3	22.8	0.3%	1.8%	1.7%
10^4	26.1	0.4%	1.5%	1.5%
10^5	29.3	0.6%	1.6%	1.5%
10^6	32.5	0.6%	1.3%	1.2%
10^7	36.3	4.9%	6.2%	4.7%
B/Utah				
Fold dilution	*Observed GMCt*	*Repeatability*	*Intermediate precision*	*Format variability*
10^0	12.4	1.1%	4.4%	4.3%
10^1	15.6	0.4%	3.6%	3.5%
10^2	18.9	0.3%	2.9%	2.9%
10^3	22.2	0.2%	2.5%	2.5%
10^4	25.5	0.2%	2.2%	2.2%
10^5	28.8	0.6%	2.0%	1.9%
10^6	32.1	0.5%	1.7%	1.6%
10^7	35.2	1.2%	2.4%	2.2%
B/Mass				
Fold dilution	*Observed GMCt*	*Repeatability*	*Intermediate precision*	*Format variability*
10^0	13.9	0.7%	1.4%	1.3%
10^1	17.1	0.3%	1.2%	1.2%
10^2	20.3	0.3%	1.0%	1.0%
10^3	23.6	0.3%	0.9%	0.9%
10^4	26.7	0.3%	0.8%	0.8%
10^5	30.5	0.4%	3.5%	3.5%
10^6	32.9	0.4%	0.6%	0.5%
10^7	36.2	3.8%	5.7%	4.7%

12. BIBLIOGRAPHY

1. Influenza Virus. (2009). Transfusion Medicine and Hemotherapy, 36(1), 32–39. https://doi.org/10.1159/000197314

2. Kumar, B., Asha, K., Khanna, M., Ronsard, L., Meseko, C., & Sanicas, M. (2018). The emerging influenza virus threat: status and new prospects for its therapy and control. Archives of Virology, 163(4), 831–844. https://doi.org/10.1007/s00705-018-3708-y

3. Wolff, T., & Veit, M. (2021). Influenza B, C and D Viruses (Orthomyxoviridae). In Elsevier eBooks (pp. 561–574). https://doi.org/10.1016/b978-0-12-809633-8.21505-7

4. Van De Sandt, C. E., Bodewes, R., Rimmelzwaan, G. F., & De Vries, R. D. (2015). Influenza B viruses: not to be discounted. Future Microbiology, 10(9), 1447–1465. https://doi.org/10.2217/fmb.15.65

5. Collin, E. A., Sheng, Z., Lang, Y., Liu, T., Hause, B. M., & Li, F. (2015). Cocirculation of Two Distinct Genetic and Antigenic Lineages of Proposed Influenza D Virus in Cattle. Journal of Virology, 89(2), 1036–1042. https://doi.org/10.1128/jvi.02718-14

6. Trombetta, C. M., Marchi, S., Manini, I., Kistner, O., Li, F., Piu, P., Manenti, A., Biuso, F., Sreenivasan, C., Druce, J., & Montomoli, E. (2019). Influenza D Virus: Serological Evidence in the Italian Population from 2005 to 2017. Viruses, 12(1), 30. https://doi.org/10.3390/v12010030

7. Krammer, F., Smith, G. J. D., Fouchier, R. a. M., Peiris, J. S. M., Kedzierska, K., Doherty, P. C., Palese, P., Shaw, M. L., Treanor, J. J., Webster, R. G., & García-Sastre, A. (2018). Influenza. Nature Reviews Disease Primers, 4(1). https://doi.org/10.1038/s41572-018-0002-y

8. Dharmapalan, D. (2020). Influenza. Indian Journal of Pediatrics, 87(10), 828–832. https://doi.org/10.1007/s12098-020-03214-1

9. World Health Organization (WHO). (1980). A revised system for nomenclature of Influenza viruses. Bull World Health Organization. 58: 585-591.

10. Fodor, E., & Velthuis, A. J. W. T. (2019). Structure and Function of the Influenza Virus Transcription and Replication Machinery. Cold Spring Harbor Perspectives in Medicine, 10(9), a038398. https://doi.org/10.1101/cshperspect.a038398

11. Eisfeld, A. J., Neumann, G., & Kawaoka, Y. (2014). At the centre: influenza A virus ribonucleoproteins. Nature Reviews Microbiology, 13(1), 28–41. https://doi.org/10.1038/nrmicro3367

12. Influenza Type A Viruses. (2023, April 28). Centers for Disease Control and Prevention. https://www.cdc.gov/flu/avianflu/influenza-a-virus-subtypes.htm

13. Klimov, A., Garten, R., Russell, C. A., Barr, I. G., Besselaar, T. G., Daniels, R. S., Engelhardt, O. G., Grohmann, G., Itamura, S., Kelso, A., McCauley, J. W., Odagiri, T., Smith, D. R., Tashiro, M., Xu, X., Webby, R. J., Wang, D., Ye, Z., Yuelong, S., . . . Cox, N. J. (2012). WHO recommendations for the viruses to be used in the 2012 Southern Hemisphere Influenza Vaccine: Epidemiology, antigenic and genetic characteristics of influenza A(H1N1)pdm09, A(H3N2) and B influenza viruses collected from February to September 2011. Vaccine, 30(45), 6461–6471. https://doi.org/10.1016/j.vaccine.2012.07.089

14. Paget, J., Caini, S., Del Riccio, M., Van Waarden, W., & Meijer, A. (2022). Has influenza B/Yamagata become extinct and what implications might this have for quadrivalent influenza vaccines? Eurosurveillance, 27(39). https://doi.org/10.2807/1560-7917.es.2022.27.39.2200753

15. How Flu Viruses Can Change. (2022, December 12). Centers for Disease Control and Prevention. https://www.cdc.gov/flu/about/viruses/change.htm

16. Gamblin, S. J., Vachieri, S., Xiong, X., Zhang, J., Martin, S. F., & Skehel, J. J. (2020). Hemagglutinin Structure and Activities. Cold Spring Harbor Perspectives in Medicine, 11(10), a038638. https://doi.org/10.1101/cshperspect.a038638

17. Wiley, D. C., & Skehel, J. J. (1987). THE STRUCTURE AND FUNCTION OF THE HEMAGGLUTININ MEMBRANE GLYCOPROTEIN OF INFLUENZA VIRUS. Annual Review of Biochemistry, 56(1), 365–394. https://doi.org/10.1146/annurev.bi.56.070187.002053

18. McAuley, J. L., Gilbertson, B., Trifkovic, S., Brown, L. E., & McKimm-Breschkin, J. L. (2019). Influenza Virus Neuraminidase Structure and Functions. Frontiers in Microbiology, 10. https://doi.org/10.3389/fmicb.2019.00039

19. Burnet, F. M. (1948). Mucins and mucoids in relation to influenza virus action; inhibition of virus haemagglutination by glandular mucins. Aust. J. Exp. Biol. Med. Sci. 26, 371–379. doi: 10.1038/icb.1948.38

20. Lentz, M. R., Webster, R. G., and Air, G. M. (1987). Site-directed mutation of the active site of influenza neuraminidase and implications for the catalytic mechanism. Biochemistry 26, 5351–5358.

21. Samji, T. (2009, December 1). Influenza A: Understanding the Viral Life Cycle. PubMed Central (PMC). https://www.ncbi.nlm.nih.gov/pmc/articles/PMC2794490/#:~:text=The%20influenza%20virus%20life%20cycle,the%20host%20cell%20plasma%20membrane

22. Pinto LH, Lamb RA. The M2 proton channels of influenza A and B viruses. J Biol Chem. 2006;281(14):8997–9000

23. Shim, J. Y., Kim, J., Tenson, T., Min, J., & Kainov, D. E. (2017). Influenza Virus Infection, Interferon Response, Viral Counter-Response, and Apoptosis. Viruses, 9(8), 223. https://doi.org/10.3390/v9080223

24. Manenti, A., Maciola, A. K., Trombetta, C. M., Kistner, O., Casa, E., Hyseni, I., Razzano, I., Torelli, A., & Montomoli, E. (2020). Influenza Anti-Stalk Antibodies: Development of a New Method for the Evaluation of the Immune Responses to Universal Vaccine. Vaccines, 8(1), 43. https://doi.org/10.3390/vaccines8010043

25. Bridges, C. B., Kuehnert, M. J., & Hall, C. B. (2003). Transmission of Influenza: Implications for Control in Health Care Settings. Clinical Infectious Diseases, 37(8), 1094–1101. https://doi.org/10.1086/378292

26. Ghebrehewet, S., MacPherson, P., & Ho, A. (2016). Influenza. BMJ, i6258. https://doi.org/10.1136/bmj.i6258

27. Klenk HD, Matrosovich M, Stech J (2008). "Avian Influenza: Molecular Mechanisms of Pathogenesis and Host Range". In Mettenleiter TC, Sobrino F (eds.). Animal Viruses: Molecular Biology. Caister Academic Press. ISBN 978-1-904455-22-6.

28. St Mouritz AA (1921). 'The Flu' A Brief World History of Influenza. Honolulu: Advertiser Publishing Co., Ltd. Retrieved 6 April 2020.

29. Hilleman MR (August 2002). "Realities and enigmas of human viral influenza: pathogenesis, epidemiology and control". Vaccine. 20 (25–26): 3068–87. doi:10.1016/S0264-410X(02)00254-2. PMID 12163258

30. World Health Organization (May 2022). "Vaccines against influenza: WHO position paper – May 2022". Weekly Epidemiological Record. 97 (19): 185–208. hdl:10665/354265.

31. Implementation of the Council Recommendation on seasonal influenza vaccination. (2014, January 9). European Centre for Disease Prevention and Control. https://www.ecdc.europa.eu/en/publications-data/implementation-council-recommendation-seasonal-influenza-vaccination

32. Seasonal Flu Vaccines | CDC. (n.d.). https://www.cdc.gov/flu/prevent/flushot.htm

33. Ferdinands, J. M., Thompson, M. C., Blanton, L., Spencer, S. J., Grant, L. N., & Fry, A. M. (2021). Does influenza vaccination attenuate the severity of breakthrough infections? A narrative review and recommendations for further research. Vaccine, 39(28), 3678–3695. https://doi.org/10.1016/j.vaccine.2021.05.011

34. Olson, S. M., Newhams, M. M., Halasa, N. B., Feldstein, L. R., Novak, T., Weiss, S. T., Coates, B. M., Schuster, J. E., Schwarz, A. J., Maddux, A. B., Hall, M. A., Nofziger, R., Flori, H. R., Gertz, S. J., Kong, M., Sanders, R. C., Irby, K., Hume, J. R., Cullimore, M. L., . . . Randolph, A. G. (2022). Vaccine Effectiveness Against Life-Threatening Influenza Illness in US Children. Clinical Infectious Diseases, 75(2), 230–238. https://doi.org/10.1093/cid/ciab931

35. Crowe JE. Chapter 260 Respiratory Syncytial Virus. 2016.

36. Griffiths C, Drews SJ, Marchant DJ (January 2017). "Respiratory Syncytial Virus: Infection, Detection, and New Options for Prevention and Treatment". Clinical Microbiology Reviews. 30 (1): 277–319. doi:10.1128/CMR.00010-16. PMC 5217795. PMID 27903593.

37. Coultas JA, Smyth R, Openshaw PJ (October 2019). "Respiratory syncytial virus (RSV): a scourge from infancy to old age". Thorax. 74 (10): 986–993. doi:10.1136/thoraxjnl-2018-212212. PMID 31383776. S2CID 199449874.

38. Pandya, M. C., Callahan, S. J., Savchenko, K. G., & Stobart, C. C. (2019). A Contemporary View of Respiratory Syncytial Virus (RSV) Biology and Strain-Specific Differences. Pathogens, 8(2), 67. https://doi.org/10.3390/pathogens8020067

39. Ramilo O, Rodriguez-Fernandez R, Mejias A. Respiratory Syncytial Virus (RSV) Infection: Old Challenges and New Approaches. J Infect Dis. 2023.

40. Bonifazi, C, Trombetta, CM, Barneschi, I, et al. Establishment and validation of a high-throughput micro-neutralization assay for respiratory syncytial virus (subtypes A and B). J Med Virol. 2023; 95:e28923. doi:10.1002/jmv.28923.

41. Collins, P. L., Fearns, R., & Graham, B. S. (2013). Respiratory Syncytial Virus: Virology, Reverse Genetics, and Pathogenesis of Disease. In Springer eBooks (pp. 3–38). https://doi.org/10.1007/978-3-642-38919-1_1

42. Collins PL, Mottet G. Oligomerization and post-translational processing of glycoprotein G of human respiratory syncytial virus: altered O-glycosylation in the presence of brefeldin A. J Gen Virol. 1992;73(4):849–863.

43. McLellan, J. S., Ray, W. J., & Peeples, M. E. (2013). Structure and Function of Respiratory Syncytial Virus Surface Glycoproteins. In Current Topics in Microbiology and Immunology (pp. 83–104). Springer Science+Business Media. https://doi.org/10.1007/978-3-642-38919-1_4

44. Mejias, A., Garcia-Maurino, C., Rodríguez-Fernández, R., Peeples, M. E., & Ramilo, O. (2017). Development and clinical applications of novel antibodies for prevention and treatment of respiratory syncytial virus infection. Vaccine, 35(3), 496–502. https://doi.org/10.1016/j.vaccine.2016.09.026

45. Graham, B. S. (2019). Immunological goals for respiratory syncytial virus vaccine development. Current Opinion in Immunology, 59, 57–64. https://doi.org/10.1016/j.coi.2019.03.005

46. Andreano, E., Paciello, I., Bardelli, M., Tavarini, S., Sammicheli, C., Frigimelica, E., Guidotti, S., Torricelli, G., Biancucci, M., D'Oro, U., Chandramouli, S., Bottomley, M. J., Rappuoli, R., Finco, O., & Buricchi, F. (2021). The respiratory syncytial virus (RSV) prefusion F-protein functional antibody repertoire in adult healthy donors. Embo Molecular Medicine, 13(6). https://doi.org/10.15252/emmm.202114035

47. Bakker, S., Duquerroy, S., Galloux, M., Loney, C., Conner, E. R., Eléouët, J., Rey, F. A., & Bhella, D. (2013). The respiratory syncytial virus nucleoprotein–RNA complex forms a left-handed helical nucleocapsid. Journal of General Virology, 94(8), 1734–1738. https://doi.org/10.1099/vir.0.053025-0

48. Zhang, L.; Peeples, M.E.; Boucher, R.C.; Collins, P.L.; Pickles, R.J. Respiratory syncytial virus infection of human airway epithelial cells is polarized, specific to ciliated cells, and without obvious cytopathology. J. Virol. 2002, 76, 5654–5666

49. Cowton VM, McGivern DR, Fearns R (July 2006). "Unravelling the complexities of respiratory syncytial virus RNA synthesis". The Journal of General Virology. 87 (Pt 7): 1805–1821. doi:10.1099/vir.0.81786-0. PMID 16760383.

50. RSV Transmission. (2023, April 26). Centers for Disease Control and Prevention. https://www.cdc.gov/rsv/about/transmission.html

51. Azzari, C., Baraldi, E., Bonanni, P., Bozzola, E., Coscia, A., Lanari, M., Manzoni, P., Mazzone, T., Sandri, F., Lisi, G. C., Parisi, S., Piacentini, G., & Mosca, F. (2021). Epidemiology and prevention of respiratory syncytial virus infections in children in Italy. Italian Journal of Pediatrics, 47(1). https://doi.org/10.1186/s13052-021-01148-8

52. Jha, A. (2016b, June 1). Respiratory Syncytial Virus. SARS, MERS and Other Viral Lung Infections - NCBI Bookshelf. https://www.ncbi.nlm.nih.gov/books/NBK442240/

53. Falsey, A. R., & Walsh, E. E. (2000). Respiratory Syncytial Virus Infection in Adults. Clinical Microbiology Reviews, 13(3), 371–384. https://doi.org/10.1128/cmr.13.3.371-384.2000

54. Bsn, R. Z. R. (2021, December 6). Examining the seasonal shift of RSV. Contemporary Pediatrics. https://www.contemporarypediatrics.com/view/examining-the-seasonal-shift-of-rsv

55. Romero, J. R. (2003). Palivizumab prophylaxis of respiratory syncytial virus disease from 1998 to 2002: results from four years of palivizumab usage. Pediatric Infectious Disease Journal, 22(Supplement), S46–S54. https://doi.org/10.1097/01.inf.0000053885.34703.84

56. Drysdale, S. B., Green, C. J., & Sande, C. J. (2016). Best practice in the prevention and management of paediatric respiratory syncytial virus infection. Therapeutic Advances in Infectious Disease, 3(2), 63–71. https://doi.org/10.1177/2049936116630243

57. Office of the Commissioner. (2023). FDA Approves First Respiratory Syncytial Virus (RSV) Vaccine. U.S. Food And Drug Administration. https://www.fda.gov/news-events/press-announcements/fda-approves-first-respiratory-syncytial-virus-rsv-vaccine

58. U.S. FDA Approves ABRYSVOTM, Pfizer's Vaccine for the Prevention of Respiratory Syncytial Virus (RSV) in Older Adults | Pfizer. (n.d.). https://www.pfizer.com/news/press-release/press-release-detail/us-fda-approves-abrysvotm-pfizers-vaccine-prevention#:~:text=(NYSE%3A%20PFE)%20announced%20today,individuals%2060%20years%20and%20older

59. Mohammad Mahdi Moein, Aziza El Beqqali, Mohamed Abdel-Rehim, Bioanalytical method development and validation: critical concepts and strategies, Journal of Chromatography B http://dx.doi.org/10.1016/j.jchromb.2016.09.028

60. European Medicines Agency. ICH Q2(R2) Validation of analytical procedures - Scientific guideline. 2022.

61. U.S. Food And Drug Administration. M10 Bioanalytical Method Validation and Study Sample Analysis. https://www.fda.gov/regulatory-information/search-fda-guidance-documents/m10-bioanalytical-method-validation-and-study-sample-analysis

62. Andreasson, U., Perret-Liaudet, A., Van Waalwijk Van Doorn, L. J. C., Blennow, K., Chiasserini, D., Engelborghs, S., Fladby, T., Genc, S., Kruse, N., Kuiperij, H. B., Kulic, L., Lewczuk, P., Mollenhauer, B., Mroczko, B., Parnetti, L., Vanmechelen, E., Verbeek, M. M.,

Winblad, B., Zetterberg, H., . . . Teunissen, C. E. (2015). A practical guide to immunoassay method validation. Frontiers in Neurology, 6. https://doi.org/10.3389/fneur.2015.00179

63. Plotkin, S. A. (2023). Recent updates on correlates of vaccine-induced protection. Frontiers in Immunology, 13. https://doi.org/10.3389/fimmu.2022.1081107

64. Hobson, D., Curry, R. L., Beare, A., & Ward-Gardner, A. (1972). The role of serum haemagglutination-inhibiting antibody in protection against challenge infection with influenza A2 and B viruses. Epidemiology and Infection, 70(4), 767–777. https://doi.org/10.1017/s0022172400022610

65. Trombetta CM, Montomoli E. Influenza immunology evaluation and correlates of protection: a focus on vaccines. Expert Rev Vaccines (2016) 15(8):967–76. doi: 10.1586/14760584.2016.1164046

66. Zhou F, Hansen L, Pedersen G, Grødeland G, Cox R. Matrix m adjuvanted H5N1 vaccine elicits broadly neutralizing antibodies and neuraminidase inhibiting antibodies in humans that correlate with In vivo protection. Front Immunol (2021) 12:747774. doi: 10.3389/fimmu.2021.747774

67. Morley, P. S., Hanson, L. C., Bogdan, J. R., Townsend, H. G., Appleton, J. A., & Haines, D. M. (1995). The relationship between single radial hemolysis, hemagglutination inhibition, and virus neutralization assays used to detect antibodies specific for equine influenza viruses. Veterinary Microbiology, 45(1), 81–92. https://doi.org/10.1016/0378-1135(94)00105-6

68. Trombetta, C. M., Perini, D., Mather, S., Temperton, N. J., & Montomoli, E. (2014). Overview of Serological Techniques for Influenza Vaccine Evaluation: Past, Present and Future. Vaccines, 2(4), 707–734. https://doi.org/10.3390/vaccines2040707

69. Johansson, B., & Cox, M. M. (2011). Influenza viral neuraminidase: the forgotten antigen. Expert Review of Vaccines, 10(12), 1683–1695. https://doi.org/10.1586/erv.11.130

70. McIlwain, D. R., Chen, H. Y. H., Rahil, Z., Bidoki, N. H., Jiang, S., Bjornson, Z., Kolhatkar, N. S., Martinez, C. J., Gaudilliere, B., Hedou, J., Mukherjee, N., Schürch, C. M., Trejo, A., Affrime, M. B., Bock, B., Kim, K. A., Liebowitz, D., Aghaeepour, N., Tucker, S. N., & Nolan,

G. P. (2021). Human influenza virus challenge identifies cellular correlates of protection for oral vaccination. Cell Host & Microbe, 29(12), 1828-1837.e5. https://doi.org/10.1016/j.chom.2021.10.009

71. Gianchecchi, E., Torelli, A., & Montomoli, E. (2019). The use of cell-mediated immunity for the evaluation of influenza vaccines: an upcoming necessity. Human Vaccines & Immunotherapeutics, 15(5), 1021–1030. https://doi.org/10.1080/21645515.2019.1565269

72. Buchwald, A. G., Graham, B. S., Traore, A., Haidara, F. C., Chen, M., Morabito, K. M., Lin, B. C., Sow, S. O., Levine, M. M., Pasetti, M. F., & Tapia, M. D. (2020). Respiratory Syncytial Virus (RSV) Neutralizing Antibodies at Birth Predict Protection from RSV Illness in Infants in the First 3 Months of Life. Clinical Infectious Diseases, 73(11), e4421–e4427. https://doi.org/10.1093/cid/ciaa648

73. Fong, Y., Huang, Y., Borate, B., Van Der Laan, L., Zhang, W., Carpp, L. N., Cho, I., Glenn, G., Fries, L., Gottardo, R., & Gilbert, P. B. (2023). Antibody Correlates of Protection From Severe Respiratory Syncytial Virus Disease in a Vaccine Efficacy Trial. Open Forum Infectious Diseases, 10(1). https://doi.org/10.1093/ofid/ofac693

74. Kulkarni PS, Hurwitz JL, Simões EAF, Piedra PA. Establishing Correlates of Protection for Vaccine Development: Considerations for the Respiratory Syncytial Virus Vaccine Field. Viral Immunol. 2018 Mar;31(2):195-203. doi: 10.1089/vim.2017.0147. Epub 2018 Jan 16. PMID: 29336703; PMCID: PMC5863081.

75. Gianchecchi, E., Torelli, A., Piu, P., Bonifazi, C., Ganfini, L., & Montomoli, E. (2023). Flow cytometry as an integrative method for the evaluation of vaccine immunogenicity: A validation approach. Biochemistry and Biophysics Reports, 34, 101472. https://doi.org/10.1016/j.bbrep.2023.101472

76. Selliah, N., Eck, S., Green, C., Oldaker, T., Stewart, J. L., Vitaliti, A., & Litwin, V. (2018). Flow Cytometry Method Validation Protocols. Current Protocols in Cytometry, 87(1), e53. https://doi.org/10.1002/cpcy.53

77. McKinnon, K. (2018). Flow Cytometry: An Overview. Current Protocols in Immunology, 120(1). https://doi.org/10.1002/cpim.40

78. Picot, J., Guerin, C. L., Van Kim, C. L., & Boulanger, C. M. (2012). Flow cytometry: retrospective, fundamentals and recent instrumentation. Cytotechnology, 64(2), 109–130. https://doi.org/10.1007/s10616-011-9415-0

79. Marshall, J.S., Warrington, R., Watson, W. et al. An introduction to immunology and immunopathology. Allergy Asthma Clin Immunol 14 (Suppl 2), 49 (2018). https://doi.org/10.1186/s13223-018-0278-1

80. Janeway, Charles; Travers, Paul; Walport, Mark; Shlomchik, Mark (2001). Immunobiology (5th ed.). New York: Garland Science. ISBN 978-0-8153-3642-6

81. Romagnani S. Th1/Th2 cells. Inflamm Bowel Dis. 1999 Nov;5(4):285-94. doi: 10.1097/00054725-199911000-00009. PMID: 10579123.

82. Al-Shura AN (2020). "Lymphocytes". Advanced Hematology in Integrated Cardiovascular Chinese Medicine. Elsevier. pp. 41–46. doi:10.1016/b978-0-12-817572-9.00007-0. ISBN 978-0-12-817572-9. S2CID 241913878

83. Punnonen, J., Aversa, G., Cocks, B. G., McKenzie, A. N. J., Menon, S., Zurawski, S., De Waal Malefyt, R., & De Vries, J. A. (1993). Interleukin 13 induces interleukin 4-independent IgG4 and IgE synthesis and CD23 expression by human B cells. Proceedings of the National Academy of Sciences of the United States of America, 90(8), 3730–3734. https://doi.org/10.1073/pnas.90.8.3730

84. De Rosa S.C., Edupuganti S., Huang Y., Han X., Elizaga M., Swann E., Polakowski L., Kalams S.A., Keefer M.C., Maenza J., Lu Y., Wise M.C., Yan J., Morrow M.P., Khan A.S., Boyer J.D., Humeau L., White S., Pensiero M., Sardesai N.Y., Bagarazzi M.L., Weiner D.B., Ferrari G., Tomaras G.D., Montefiori D.C., Corey L., McElrath M.J. HIV Vaccine Trials Network (HVTN) 098 Study Team. Robust antibody and cellular responses induced by DNA-only vaccination for HIV. JCI Insight. 2020;5 doi: 10.1172/jci.insight.137079

85. Otani N., Shima M., Ueda T., Ichiki K., Nakajima K., Takesue Y., Okuno T. Evaluation of influenza vaccine-immunogenicity in cell-mediated immunity. Cell. Immunol. 2016;310:165–169. doi: 10.1016/j.cellimm.2016.09.005

86. Price L.S., Adamow M., Attig S., Fecci P., Norberg P., Reap E., Janetzki S., McNeil L.K. Gating harmonization guidelines for intracellular cytokine staining validated in second international multiconsortia proficiency panel conducted by cancer immunotherapy consortium (CIC/CRI) Cytometry. 2021;99:107–116.

87. Uhlen M., Bandrowski A., Carr S., Edwards A., Ellenberg J., Lundberg E., L Rimm D., Rodriguez H., Hiltke T., Snyder M., Yamamoto T. A proposal for validation of antibodies. Nat. Methods. 2016;13:823–827. doi: 10.1038/nmeth.3995

88. Organization, W. H., & Network, W. G. I. S. (2011). Manual for the Laboratory Diagnosis and Virological Surveillance of Influenza.

89. Freeman, W. M., Walker, S. G., & Vrana, K. E. (1999). Quantitative RT-PCR: pitfalls and potential. BioTechniques, 26(1), 112–125. https://doi.org/10.2144/99261rv01

90. Deoxynucleotide triphosphates and buffer components. (2008). In Springer eBooks (pp. 91–101). https://doi.org/10.1007/978-1-4020-6241-4_6

91. Juskowiak, B. (2010). Nucleic acid-based fluorescent probes and their analytical potential. Analytical and Bioanalytical Chemistry, 399(9), 3157–3176. https://doi.org/10.1007/s00216-010-4304-5

92. Polymerase chain Reaction (PCR). (n.d.). http://www.ncbi.nlm.nih.gov/probe/docs/techpcr/

93. Wacker, M. J., and Godard M. P. (2005). Analysis of One-Step and Two-Step Real-Time RT-PCR Using SuperScript III. Journal of Biomolecular Techniques 16(3): 266–271

94. Deepak, S. A., Kottapalli, K. R., Rakwal, R., Oros, G., Rangappa, K. S., Iwahashi, H., Masuo, Y., & Agrawal, G. P. (2007). Real-Time PCR: Revolutionizing detection and expression analysis of genes. Current Genomics, 8(4), 234–251. https://doi.org/10.2174/138920207781386960

95. World Health Organization (February 2021). “WHO information for the molecular detection of influenza viruses”.

96. Broeders, S., Huber, I., Grohmann, L., Berben, G., Taverniers, I., Mazzara, M., Roosens, N. H. C., & Morisset, D. (2014). Guidelines for validation of qualitative real-time PCR methods. Trends in Food Science and Technology, 37(2), 115–126. https://doi.org/10.1016/j.tifs.2014.03.008

97. Pachucki, C. T., Khurshid, M. A., & Nawrocki, J. (2004c). Utility of Reverse Transcriptase PCR for Rapid Diagnosis of Influenza A Virus Infection and Detection of Amantadine-Resistant Influenza A Virus Isolates. Journal of Clinical Microbiology, 42(6), 2796–2798. https://doi.org/10.1128/jcm.42.6.2796-2798.2004

98. Boivin, G., Côté, S., Déry, P., De Serres, G., & Bergeron, M. G. (2004). Multiplex Real-Time PCR Assay for Detection of Influenza and Human Respiratory Syncytial Viruses. Journal of Clinical Microbiology, 42(1), 45–51. https://doi.org/10.1128/jcm.42.1.45-51.2004

99. Stephenson, I., Das, R. G., Wood, J. N., & Katz, J. M. (2007). Comparison of neutralising antibody assays for detection of antibody to influenza A/H3N2 viruses: An international collaborative study. Vaccine, 25(20), 4056–4063. https://doi.org/10.1016/j.vaccine.2007.02.039

100. Martínez, I., Lombardia, L., Herranz, C., García-Barreno, B., Domínguez, O., & Melero, J. A. (2009). Cultures of HEp-2 cells persistently infected by human respiratory syncytial virus differ in chemokine expression and resistance to apoptosis as compared to lytic infections of the same cell type. Virology, 388(1), 31–41. https://doi.org/10.1016/j.virol.2009.03.008

101. Kwilas, S. A., Liesman, R. M., Zhang, L., Walsh, E. E., Pickles, R. J., & Peeples, M. E. (2009). Respiratory syncytial virus grown in Vero cells contains a truncated attachment protein that alters its infectivity and dependence on glycosaminoglycans. Journal of Virology, 83(20), 10710–10718. https://doi.org/10.1128/jvi.00986-09

102. Ausar, S. F., Espina, M., Brock, J., Thyagarayapuran, N., Repetto, R., Khandke, L., & Middaugh, C. R. (2007). High-throughput screening of stabilizers for Respiratory Syncytial Virus: Identification of stabilizers and their effects on the conformational thermostability of viral particles. Human Vaccines, 3(3), 94–103. https://doi.org/10.4161/hv.3.3.4149